AD-A077 335 PENNSYLVANIA STATE UNIV UNIVERSITY PARK ORDNANCE RES--ETC F/G 20/4
THE ORL FLUIDS ENGINEERING UNIT AXIAL FLOW RESEARCH FAN.(U)
JUN 72 E P BRUCE N00017-70-C-1407
UNCLASSIFIED TM-72-109 NL

1 OF 1
AD-
A077335

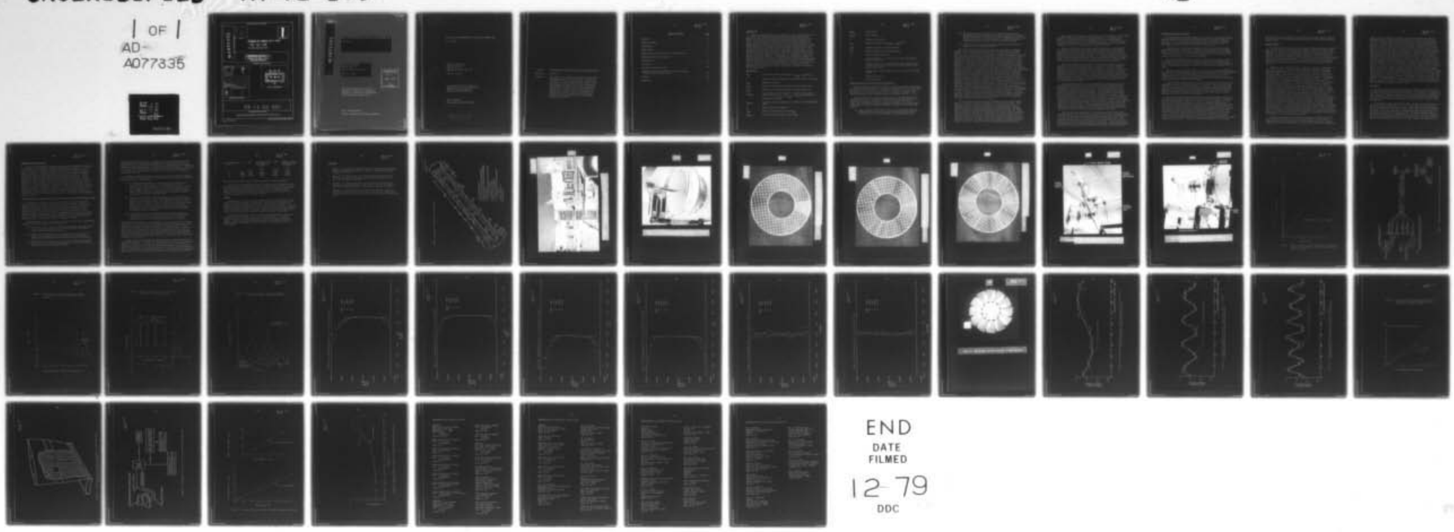

END
DATE
FILMED
12-79
DDC

PHOTOGRAPH THIS SHEET

AD A077335

DTIC ACCESSION NUMBER

II

LEVEL

INVENTORY

Contract No. N00017-70-C-1407

TM-72-109

DOCUMENT IDENTIFICATION

DISTRIBUTION STATEMENT A

Approved for public release;
Distribution Unlimited

DISTRIBUTION STATEMENT

ACCESSION FOR	
NTIS GRA&I	☒
DTIC TAB	☐
UNANNOUNCED	☐
JUSTIFICATION	
BY	
DISTRIBUTION /	
AVAILABILITY CODES	
DIST	AVAIL AND/OR SPECIAL
A	

DISTRIBUTION STAMP

DDC
RECEIVED
NOV 29 1979
D

DATE ACCESSIONED

79 11 23 539

DATE RECEIVED IN DTIC

PHOTOGRAPH THIS SHEET AND RETURN TO DTIC-DDA-2

DTIC FORM OCT 79 70A

DOCUMENT PROCESSING SHEET

THE ORL FLUIDS ENGINEERING UNIT AXIAL FLOW RESEARCH FAN

E. P. Bruce

Technical Memorandum
File No. TM 72-109
June 22, 1972
Contract No. N00017-70-C-1407

Copy No. 18

The Pennsylvania State University
Institute for Science and Engineering
ORDNANCE RESEARCH LABORATORY
University Park, Pennsylvania

NAVY DEPARTMENT

NAVAL ORDNANCE SYSTEMS COMMAND

THE ORL FLUIDS ENGINEERING UNIT AXIAL FLOW RESEARCH FAN

E. P. Bruce

Technical Memorandum
File No. TM 72-109
June 22, 1972
Contract No. N00017-70-C-1407

Copy No. 18

The Pennsylvania State University
Institute for Science and Engineering
ORDNANCE RESEARCH LABORATORY
University Park, Pennsylvania

NAVY DEPARTMENT

NAVAL ORDNANCE SYSTEMS COMMAND

Subject: The ORL Fluids Engineering Unit Axial Flow Research Fan

References: See Page 13

Abstract: A description of the ORL Fluids Engineering unit Axial Flow Research Fan is presented herein. The size and flexibility of this facility are such as to provide a previously unavailable capability for research on the time-dependent response of axial flow turbomachinery blade elements and blade rows to time or spatially varying flows. Flows of this type are generated by interaction of adjacent blade rows or by blade row response to a distorted inflow. Consequently, an understanding of the phenomena that govern blade response in these environments is of considerable practical significance.

TABLE OF CONTENTS

INTRODUCTION

A major technical problem in the reduction of noise and vibration from all classes of turbomachines rests at the source itself, namely at the compressor, pump, fan or propeller which is used to supply energy to the fluid. All of these devices generate undesirable sound and vibration due to the same basic phenomena - the response of parts of the machine to a temporally and spatially non-uniform flow. The widespread exposure to these machines has led to an upsurge in public awareness of the deleterious effect on the environment of turbomachinery generated noise and vibration. This in turn has led to legislative control. The present interpretation of the generation of pollution of this type is derived by analysis from calculated results based on the application of unsteady isolated airfoil theory. This theory has not been checked in this application. Consequently, the results obtained are open to question. The ORL Axial Flow Research Fan (AFRF) was designed specifically to provide a capability for detailed research which will define the response of axial flow turbomachinery blade elements and/or blade rows to unsteady flows of the type encountered in practice. Consequently, it provides a unique capability for the generation of design data and for phenomenological studies whose results can be used to evaluate the adequacy of theoretical models.

NOMENCLATURE

Cp_{T_L}	Local total pressure coefficient, $(p_{T_{LOCAL}} - p_{ATM})/q_{REF}$
N	Number of inflow disturbance cycles encountered per revolution
p_{ATM}	Atmospheric pressure
ps_{REF}	Reference static pressure measured by pitot-static tube
pT_{REF}	Reference total pressure measured by pitot-static tube
$ps_{1_{LOCAL}}$	Local static pressure measured at a station in the rotor-stator region, $ps_{1_{LOCAL}} = ps_{2_{LOCAL}} = ps_{LOCAL}$ when probe is aligned with the flow.
pT_{LOCAL}	Local total pressure measured at a station in the rotor-stator region
p_w	Outer casing static pressure
q_{REF}	Reference dynamic pressure, $1/2\rho\ V^2_{REF}$
R_{CASING}	Outer casing inside radius, 10.75 inches

R_{LOCAL}	Local radius
V_{LOCAL}	Local velocity
$\overline{V}$	Average local velocity
V_{REF}	Reference velocity, $[\frac{2}{\rho}(p_{T_{REF}} - p_{s_{REF}})]^{1/2}$
$\lvert\Delta L\rvert$	Maximum amplitude of fluctuating lift
$\lvert\Delta M\rvert$	Maximum amplitude of fluctuating moment
Δp	Static pressure difference
α	Local flow angle, $\alpha = 0$ for flow in a plane containing the facility centerline
θ	Circumferential position measured in a plane normal to the facility centerline, positive for counterclockwise rotation when looking forward.
λ	Stagger angle, angle between airfoil chord line and the axial direction
ρ	Atmospheric density
ω	Reduced frequency

GENERAL DESCRIPTION OF THE AXIAL FLOW RESEARCH FAN

The ORL Axial Flow Research Fan (AFRF) was designed and built by personnel of the Fluids Engineering unit. The facility became operational in January 1972. An artist's concept of the AFRF is presented in Figure 1, and a photograph of the facility as it appeared in October 1971 is presented in Figure 2. The facility operates in the stagnation pressure ratio range from 1.01 to 1.11.

Major sections of the AFRF are mounted on welded aluminum angle support dollies which can be moved along the longitudinal axis of the facility for configuration changes. The dollies rest on grooved wheels which run on tracks that are welded to the upper longitudinal members of the support stand. This support stand-dolly mounting arrangement was adopted for the following reasons:

(1) Major sections of the facility, such as the disturbance producing section and the test section, could be separated easily in the direction of the axis of the machine for configuration changes.

(2) The results presented in Reference (1) indicated that flow non-uniformities due to the presence of an inlet vortex would be present if the separation between the inlet and any solid boundary, such as the floor, was less than 2.15 inlet diameters. The AFRF centerline is 85-5/8-inches above the floor, which is 3.98 inlet diameters.

(3) Capability to rotate automated probes through a full 360° in the region of the test stage was desired.

The AFRF is 19-2/3 feet long and consists of an annular flow passage bounded at one end by a bellmouth inlet and at the other end by an exhaust throttle. The forward region, from the inlet to a point just upstream of the test rotor blade drive motor, is bounded by a 9.50-inch diameter cylindrical hub surface and a 21.50-inch inside diameter cylindircal outer casing. These surfaces are tapered to slightly larger diameters near the downstream end to permit housing the 70 HP test rotor drive motor inside the hub and to permit connection to the auxiliary fan outer casing. The 70 HP drive motor is strut mounted on its own dolly. The auxiliary fan is a Joy Manufacturing Company Model No. 23 1/4-14-3450 Series 1000 Axivane Fan which delivers 15,000 cubic feet of air per minute at a pressure of 3.5 inches of water gauge at its nominal operating condition. The auxiliary fan drive motor and the 70 HP motor operational characteristics can be independently regulated at any speed up to 3600 RPM through the use of two Borg Warner Model No. BW1200 Solid State Adjustable Frequency Drive inverter units. With a zero steady lift rotor of the type to be used in some of the initial research programs, the auxiliary fan will be used to provide the airflow. In this mode, two methods are available for final adjustment of the throughflow velocity: (1) frequency adjustment of the auxiliary fan drive control with fixed throttle setting, or (2) throttle position adjustment with the auxiliary fan operating at a fixed speed. Frequency adjustments are normally used with the throttle in the aft or full open position since this yields the highest throughflow velocity for a given frequency setting. A photograph of the exhaust throttle region with the throttle in the aft position is shown in Figure 3. Six inches of throttle travel is available. Throttle position is automatically set by operation of a 225 in-oz. torque Slo-Syn type SS250-1027 Driving Motor which is controlled by a Slow-Syn Present Indexer. With this system, throttle movement can be limited to a step of 1/3200 inch or can be as large as a step of 3.472 inches.

The wooden vane system that projects upstream from the bellmouth inlet, Figure 2, consists of eight 6-foot diameter 1/4-inch plywood vanes. These vanes were installed to remove rotation that could exist in air that is accelerated into the inlet from supposedly "at rest" conditions within the Garfield Thomas Water Tunnel Building where the AFRF is located. The AFRF shares a work area that measures approximately 140 x 30 x 40 feet in length, width and height, is divided into three major floor levels, contains six other research facilities whose size is comparable to that of the AFRF or larger, and has numerous doors and windows in the outside walls. Consequently, it is impossible to restrict activity in this area to achieve "totally controlled" operating conditions. The inlet anti-rotation vanes were designed as a first step in the effort to obtain controlled test conditions within the AFRF.

The bellmouth inlet measures 53-1/4 inches in outside diameter, 21-1/2 inches in inside diameter, and is made of laminated mahogany. It contains axial grooves on its periphery to permit installation of and to provide support for the anti-rotation vanes. The centerbody nose, which is visible in Figure 2, is made of aluminum in the shape of a length-to-diameter ratio 2 ellipse nose followed by a short 9-1/2 inch diameter cylindircal section.

The two 24-inch long outer casing segments positioned just downstream of the bellmouth inlet house the disturbance generating section. This 48-inch long flow path was provided to permit the development of distorted flowfields, generated by placing honeycomb, wire grid, or cylindrical rod obstructions at the forward end of the cylindrical annulus, into a desired pattern at the rotor inlet. Three disturbance generators of the wire grid type are shown in Figure 4. These grids were designed to provide a sinusoidal variation of axial velocity with a peak-to-peak variation of ±10% about a mean value of 80 ft/sec.

The section immediately downstream of the disturbance producing section houses the test rotor-stator stage and is the heart of the AFRF. Detailed photographs of this section are presented in Figure 5. The outer casing of the part of this section forward of the stator housing is free to rotate about the AFRF centerline. This segment of outer casing is supported by two large bearings, the housings for which are shown clearly in Figure 5b. Rotation is controlled manually, at present, and is accomplished by turning the wheel driven worm gear shown in Figure 5b. This capability was provided to permit rotation of casing mounted flow surveying probes, of the type shown in Figure 5a, in the circumferential direction.

The photographs in Figure 5 were taken during the shakedown test phase. Consequently, base filler blocks occupy the hub slots that would normally be occupied by rotor blades, Figure 5a, or stator blades, Figure 5b. These hub features are visible because one-half of one of the split outer casing sections was removed for these photographs. The AFRF design utilizes split outer casing and hub sections both upstream of and downstream of the stator. By interchanging split sections of different lengths, it is possible to move the stator blade row axially relative to the rotor blade row. Thus, tests with rotor-stator spacings of 3, 6, 9 or 12 inches are easily achieved. For 6-inch chord blades, these dimensions correspond to nondimensional rotor-stator spacings of from 1/2 to 2 blade chord lengths. When the stator is moved, part of the weight of the stator system is carried by cylindrical shafts that are mounted externally on the outer casing. The remainder of the weight is carried by a ball bushing system mounted in the hub. In Figure 6, the external shafts have been moved to their aft position to permit rotation of the probe.

The only components downstream of the stator at present are the 70 HP rotor drive motor, the auxiliary fan, and the throttle. These components were intentionally located at a downstream distance great enough to permit insertion of a silencer just downstream of the stator and thus upstream of the noise generating drive motors. An Industrial Acoustics Company Model No. 22 CL 44 Conic-Flow Silencer has been purchased for this purpose. This silencer will be installed as soon as the adapter hardware is fabricated. An additional silencer of this type may be located downstream of the drive motors at a future date.

INSTRUMENTATION AND DATA LOGGING

The instrumentation and data logging systems utilized in measuring reference operating conditions and mean flow properties in the rotor-stator region are described herein. These systems were developed for use during the shakedown test phase. The more sophisticated systems required for the measurement of time-dependent quantities will be described in later reports.

A United Sensor & Control Corp. modified Prandtl type pitot-static tube was used to measure reference flow conditions just downstream of the bellmouth inlet. This probe has a head that is fourteen tube diameters long. The probe total pressure, PT_{REF}, and static pressure, PS_{REF}, were used to define the AFRF reference velocity, V_{REF}, at the annulus mid-radius.

For flow property measurements in the rotor-stator region, where a check on flow angle was also desired, a United Sensor & Control Corp. two-dimensional type YC probe was used. This is a three-hole probe with a prism shaped measuring section that permits measurement of total and static pressure as well as flow angle.

The output from these probes, which is in the form of a pressure difference, was converted to voltage readings through the use of Validyne Engineering Corporation Model DP 15 0.5 PSID Variable Differential Pressure Transducers. A typical calibration record for one of these transducers is shown in Figure 6. The transducer output is linear over an applied differential pressure range in excess of the range covered in normal AFRF operation.

A block diagram showing the data acquisition and reduction system used in the shakedown test series is shown in Figure 7. The raw data from the Prandtl and Type YC probes, and data from probe position transducers, was recorded on paper tape for computerized reduction and in tabular form for inspection as each test progressed. The reduced data was presented in tabular form and in the form of plots of significant parameters as a function of non-dimensionalized radius through use of a Cal Comp 718 Flat Bed Plotter.

The probe position transducers indicate the radial and angular position of the probe used to measure flow properties in the rotor-stator region. The probe support mechanism shown in Figure 5a is a basic L. C. Smith Company unit that has been modified by ORL personnel to incorporate digital stepping motors. With the outer casing, and hence the probe, set at a fixed circumferential angle, the probe operation, both radial stepping and rotation about the probe axis to achieve probe alignment with the flow direction, is completely automatic. During the shakedown tests, radial traverses were routinely made in which total and static pressure and flow direction were recorded in radial steps of 1/4 inch, i.e., a total of 23 radial positions, in 25 minutes. Changes in probe axial position require withdrawing the probe through a hole in the outer casing, sliding the probe support mechanism axially, and inserting the probe at the desired outer casing access port. Access ports are shown in Figure 5a. These ports

are located at 1/2-inch increments in all major outer casing segments from the second section of the disturbance generating section to the section downstream of the stator.

SHAKEDOWN TESTS

The basic operational characteristics of the facility are shown in Figure 8 where the variation of reference velocity, V_{REF}, as measured by a pitot-static tube located centrally in the 6-inch wide annular passage at a point 12 inches downstream of the inlet, is presented as a function of throttle position and auxiliary fan inverter frequency. Reference velocities up to 111 ft/sec are possible. The effect of moving the throttle forward, at a given inverter frequency, is a reduction in reference velocity. The data show that there is little to be gained by considering more than 5 inches of throttle travel or by moving the throttle full open position aft in an attempt to raise the maximum reference velocity.

Additional data showing the effect of throttle position on performance is presented in Figure 9. Here the outer casing static pressure coefficient, $(p_W - p_{ATM})/q_{REF}$, where p_W is the static pressure at the outer casing (and across the annulus since there is no rotation and no reason for streamline curvature except in the vicinity of axial station 158 where the annulus walls are tapered outward), p_{ATM} is atmospheric pressure, and q_{REF} is $1/2\ \rho V_{REF}^2$, is presented as a function of axial station and throttle position. The ambient air density, ρ, is completely determined by the ambient temperature and static pressure. Station zero is the most forward point on the plywood inlet anti-rotation vanes, Figure 2. As shown in Figure 9, the static pressure decreases linearly in the constant area region downstream of the inlet and forward of Station 196 where the inlet to the auxiliary fan rotor is located, with a small perturbation where the wall taper causes area changes, and then increases downstream of the rotor to a level that is a function of the throttle position. The spread in the data point symbols in Figure 9 represents the maximum spread obtained from analysis of all the test conditions shown in Figure 8. The level of the wall pressure coefficient at the throttle entrance, Station 231, represents available excess back pressure which could be consumed upstream in disturbance generators or in other losses. The actual magnitude of the excess pressure available is shown in Figure 10 as a function of V_{REF} and throttle position. The approximate operational limit boundary was set by consideration of the sharp drop in velocity at large forward throttle positions shown in Figure 8. It is evident that reference velocities as high as 80 ft/sec could be maintained with additional losses as high as 5 or 6 inches of water due to the insertion of flow disturbance generators just downstream of the inlet. This indicates that the facility has a capability to investigate a wide variety of conditions at the test rotor-stator station.

During the shakedown tests, mean flow measurements taken near the rotor exit plane using the United Sensor & Controls Corporation Type YC probe indicated that the flow was unsteady. The fluctuations in this flow, which should be steady, were attributed to the fact that the facility was completely

open to extraneous ambient influences, and to the possibility that laminar separation could be occurring on the bellmouth. To isolate the flow within the annular region, the anti-rotation vane structure and the exhaust throttle opening were covered with a single layer of Sears, Roebuck and Company Fiberglass Insect Screen. This yielded some improvement. The anti-rotation vane structure was then altered by cutting away all wood not needed for a framework for the screening, and a single layer of 1/8-inch thick Scott Filter Foam was placed on the bellmouth surface. In addition, a 1-inch wide sandpaper boundary layer trip was placed on the bellmouth surface. Subsequent tests showed that these modifications had removed the unsteadiness. Results of tests made after these modifications were installed are shown in Figure 11. These data were taken with the facility operating at a reference velocity of 80 ft/sec and with the probe located just forward of the rotor inlet plane. The data are plotted in non-dimensional form for circumferential positions directly behind the anti-rotation vanes, $\theta = 0°$, 45°, 90° and 135°, and midway between vanes, $\theta = 337.5°$, 22.5°, 67.5° and 112.5°. The test data show that the central region of uniform flow is not as wide immediately behind the anti-rotation vanes as it is in the region between vanes. This result was expected. A minor modification which should improve this situation has been made since the data of Figure 11 was taken. This modification consisted of smoothing and filling all joints and cracks where the anti-rotation vanes mate with the bellmouth. At present, it is evident that the facility does provide a region of steady uniform flow that extends over the range $0.55 \leq (R_{LOCAL}/R_{CASING}) \leq 0.80$ or from $R_{LOCAL} = 5.9$ inches to $R_{LOCAL} = 8.6$ inches. It is hoped that the last modification, noted above, will extend this region to $R_{LOCAL} = 9.1$ inches. Tests to determine the new flow characteristics will be conducted during the summer of 1972.

TEST ROTOR

The first test rotor fabricated for use in the AFRF is unique in that it operates with no head input at design conditions. This feature was incorporated to permit investigations of unsteady flow effects in the absence of steady rotor lift. Positive or negative steady lift can be produced; however, by adjusting the auxiliary fan speed in relation to the test rotor speed. Thus, the effects on unsteady flow properties of incidence, ranging all the way to stall, can be investigated.

A photograph of this rotor with 12 blades installed is shown in Figure 12. The rotor can be assembled with 2, 3, 4, 6 or 12 blades each of which has a chord of 6 inches and a span of 5.9 inches. Thus, space-chord ratios defined at the mean radius of 7.75 inches of 4.058, 2.705, 2.029, 1.353 and 0.676 can be tested. The rotor blades have a 10% thick uncambered C1 profile which has the maximum thickness at the 33% chord point. The nominal stagger angle, λ, is 45° at the mean radius. Stagger angles of 35° and 55° can also be obtained by rotating the blades within the base attachment blocks. The rotor blades are made of Ren DC-63-64 Plastic which was cast over a metal base mounting plate.

DISTURBANCE GENERATING GRIDS

A total of six disturbance producing grids have been designed and fabricated for mounting in the AFRF inlet. The grids were designed to produce 1, 2, 3, 4, 5 or 6 cycle, ±10% amplitude, sinusoidal variations in axial velocity at the rotor inlet station. Photographs of three of the grids are shown in Figure 4. The grids consist of a support grid and an overlay layer composed of segments of screening which has programmed variations in wire and mesh size. The circumferential extent of these segments has been adjusted to provide a circumferentially varying loss in total pressure. Under ideal conditions, this segmented loss in total pressure at the screen will have mixed to form a sinusoidal variation in total pressure, and hence axial velocity, by the time the flow reaches the rotor inlet station. The extent to which this is realized is shown in Figure 13. These measurements were the first taken with the screens and do not reflect improvement in the sinusoidal nature of the flow which has been realized due to minor modifications aimed at eliminating both slight gaps and slight overlapping at overlay segment boundaries. Fourier analysis has shown that the flow is dominated by the fundamental in each case. The nominal measured amplitude variation is ±6%.

INSTRUMENTATION AND CONFIGURATION FOR INITIAL SERIES OF BLADE ELEMENT RESPONSE TESTS

This series of tests is being conducted to provide a direct measurement of fluctuating lift and moment developed on a mid-span chordwise segment of a blade on the AFRF zero mean lift rotor due to operation in velocity fields that contain a sinusoidally varying axial component. These data will be used to evaluate the adequacy of various theoretical models, such as those due to Sears (Reference 2), Horlock (Reference 3), and Naumann (Reference 4), which predict isolated airfoil response for various gust/airfoil interactions. Through relatively simple modifications in AFRF configuration and operating conditions, it will be possible to define the effect of changes in rotor space-chord ratio, reduced frequency, blade stagger angle and blade mean incidence.

The AFRF configuration for these tests is identical to the basic configuration illustrated in Figure 1 except for the following:

(1) A 1-, 2-, 3-, 4-, 5- or 6-cycle wire grid disturbance producing screen, of the type shown in Figure 4, will be mounted at the upstream end of the disturbance generating section.

(2) A rotor hub carrying 2, 3, 4, 6 or 12 blades set at 35°, 45° or 55° stagger at the mid-radius will be installed with a single blade instrumented for measurement of fluctuating lift and pitching moment.

(3) A multi-channel slip-ring unit will be installed over the rotor shaft and within the 9.50 inch diameter centerbody for transmission of power to and signals from the instrumented blade.

The range of reduced frequencies, ω, possible at zero mean incidence with the noted variations in stagger angle and number of inflow disturbance cycles, N, is shown in Figure 14 for the mid-radius location. Testing at positive incidence leads to slightly higher values of ω at otherwise identical conditions. Variations in incidence can be extended into the blade stall region. The space-chord ratios to be tested span the range from "isolated airfoil" at 4.058 to "strong blade interaction" at 0.676.

A schematic showing the features of the system that will be used to measure rotor blade section fluctuating lift and pitching moment is presented in Figure 15. The main features of this system are:

(1) A 1-inch span blade segment is cantilevered from the blade hub at the mid-chord position by means of a beam that has the lower portion of its length machined as a torque tube and the upper portion of its length machined as a force cube. The center section of the blade segment is located at the mean radius, 7.75 inches. The torque tube and force cube have been instrumented using Micro-Measurement 120 Ohm Foil Type Precision Strain Gages.

(2) The 1-inch span segment is made of magnesium to minimize mass and moment of inertia and is structurally independent of the rotor blade except for the cantilever mount. The aluminum outer portion of the blade attaches to posts on the aluminum hub section which pass through slots in the instrumented section. A clearance of 0.005 inches minimum has been specified for each mating surface for the initial measurement attempts. The magnesium segment has been mass-balanced to preclude uneven displacement.

(3) Input power and signal transmission lines will run from the rotor blade through the rotor hub to the hollow rotor shaft, downstream through the shaft to an over-shaft slip ring unit, and then out through holes drilled in the aft support fins shown in Figure 1.

An instrumentation schematic of the anticipated set-up for these tests is shown in Figure 16. The results of static and dynamic calibration tests of the torque tube/force cube sensor are shown in Figures 17 and 18, respectively. Pilot tests of this system in the AFRF are scheduled for September 1972. These tests will be initiated using the 1-cycle disturbance generating screen and a rotor speed on the order of 1200 RPM. Thus, the frequency with which the blade moves through the disturbance will be on the order of 20 cycles/sec. This frequency is low enough to avoid any complications due to the torque tube/force cube system resonance at 178 cycles/sec.

Calculations of the estimated lift and moment output have been made using the method of Reference 3 for the zero mean incidence case with a mean throughflow velocity of 80 ft/sec. A ±6% velocity variation due to the action of the disturbance producing screens was used in these calculations. The fluctuating lift was assumed to act at the quarter-chord point in making the moment estimates. This is in accord with the theory of Reference 2. The results of these calculations and the estimated strain gage output are presented in the following tabulation:

No. of Disturbance Cycles	ω	$\lvert\Delta L\rvert$	Estimated Strain Gage Output Due to $\lvert\Delta L\rvert$	$\lvert\Delta M\rvert$	Estimated Strain Gage Output Due to $\lvert\Delta M\rvert$
		oz.	volts	in.-oz.	volts
1	0.274	1.265	0.151	1.889	0.106
3	0.821	0.816	0.097	1.232	0.069
6	1.642	0.592	0.070	0.897	0.050

The level of this output voltage is large enough for accurate measurement.

When the tests described above have been completed and the validity of the test results has been determined, the task of measuring the chordwise distribution of unsteady differential pressure on the rotor will be initiated. Preliminary tests of this system and layouts of the installation have been completed. However, these tests are being held in abeyance until results from the force and moment measurement tests have been obtained.

SUMMARY

A description of the ORL Axial Flow Research Fan has been presented. This facility became operational in January 1972. The facility was designed specifically to provide a capability for detailed research which will define the response of axial flow turbomachinery blade elements and/or blade rows to unsteady flows of the type encountered in practice. Thus, it provides a unique capability for the generation of design data and for phenomenological studies whose results can be used to evaluate the adequacy of theoretical models of these flows.

The report also includes a description of the instrumentation used in the shakedown test phase and the results of the shakedown tests. In addition, certain specialized facility components and test programs are described in detail. These include the first test rotor, the flow disturbance generating grids, and the test program to measure unsteady lift and moment on a rotor blade segment.

June 22, 1972
EPB:mac

REFERENCES

1. Gorton, R. E., "Facilities and Instrumentation for Aircraft Engine Noise Studies," Transactions of the ASME, Journal of Engineering for Power, January 1967, pp. 1-12.

2. Sears, W. R., "Some Aspects of Non-Stationary Airfoil Theory and Its Practical Application," Journal of the Aeronautical Sciences, Vol. 8, No. 3, pp. 104-108, January 1941.

3. Horlock, J. H., "Fluctuating Lift Forces on Airfoils Moving Through Transverse and Chordwise Gusts," ASME Paper No. 68-FE-28, Presented at the Fluids Engineering Conference, Philadelphia, Pa., May 6-9, 1968.

4. Naumann, H., "Unsteady Airfoil Theory Applied to Cambered Blades and to Blade Rows of High Solidity," Ph.D. Thesis submitted to the Faculty of the Graduate School of Arts and Sciences of the University of Pennsylvania, 1971.

Figure 1. Schematic of ORL Axial Flow Research Fan

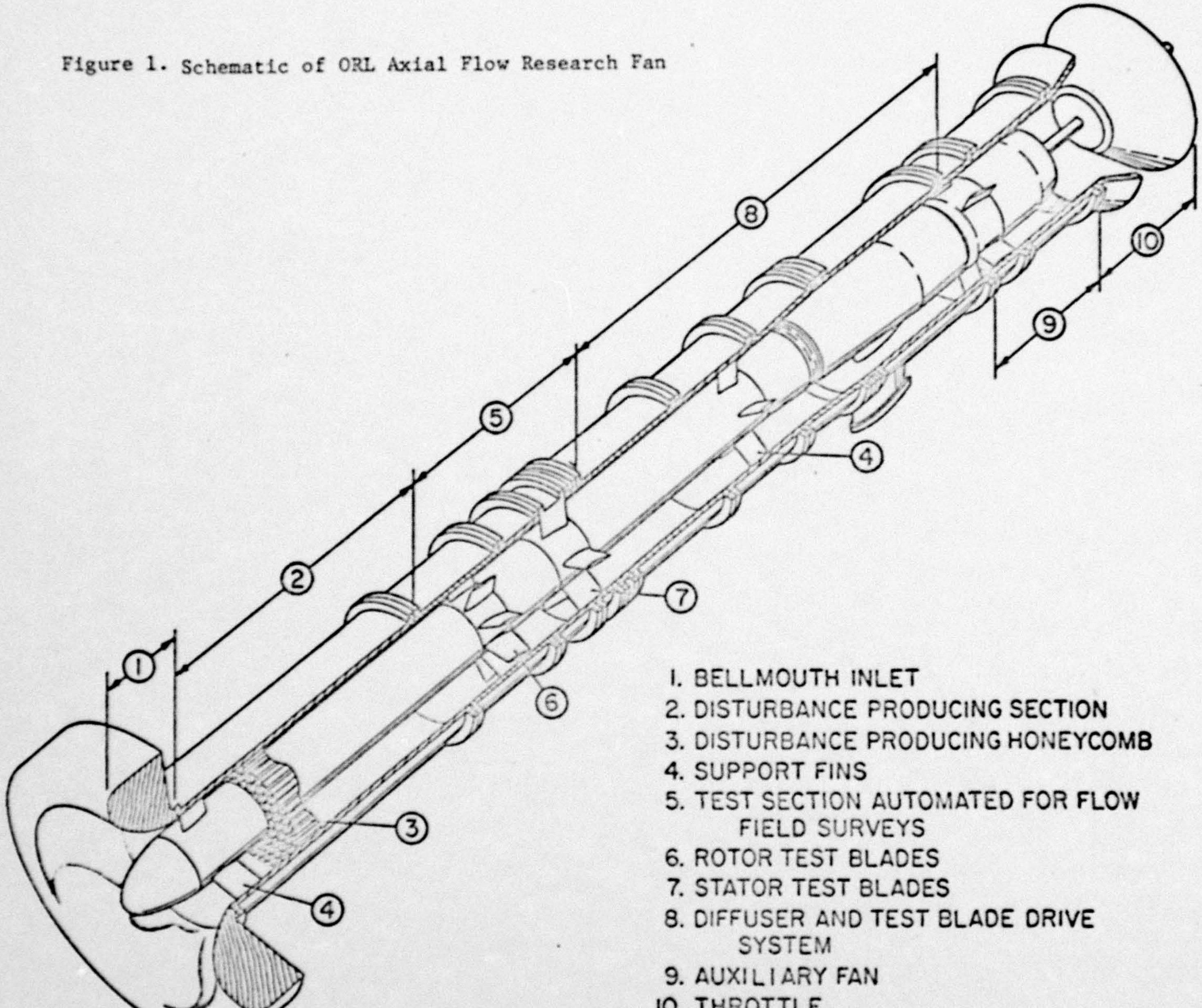

1. BELLMOUTH INLET
2. DISTURBANCE PRODUCING SECTION
3. DISTURBANCE PRODUCING HONEYCOMB
4. SUPPORT FINS
5. TEST SECTION AUTOMATED FOR FLOW FIELD SURVEYS
6. ROTOR TEST BLADES
7. STATOR TEST BLADES
8. DIFFUSER AND TEST BLADE DRIVE SYSTEM
9. AUXILIARY FAN
10. THROTTLE

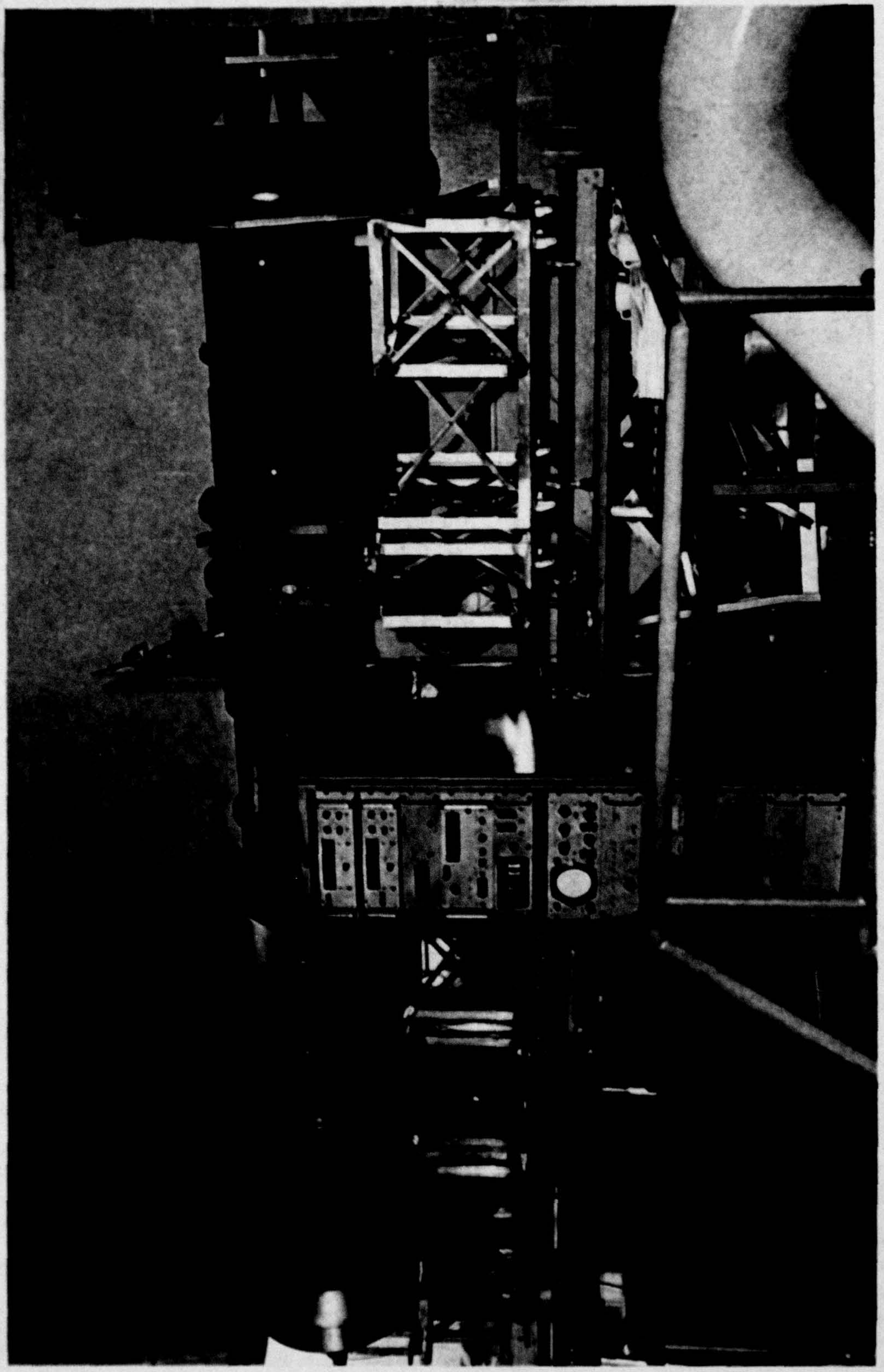

[redacted] [redacted]

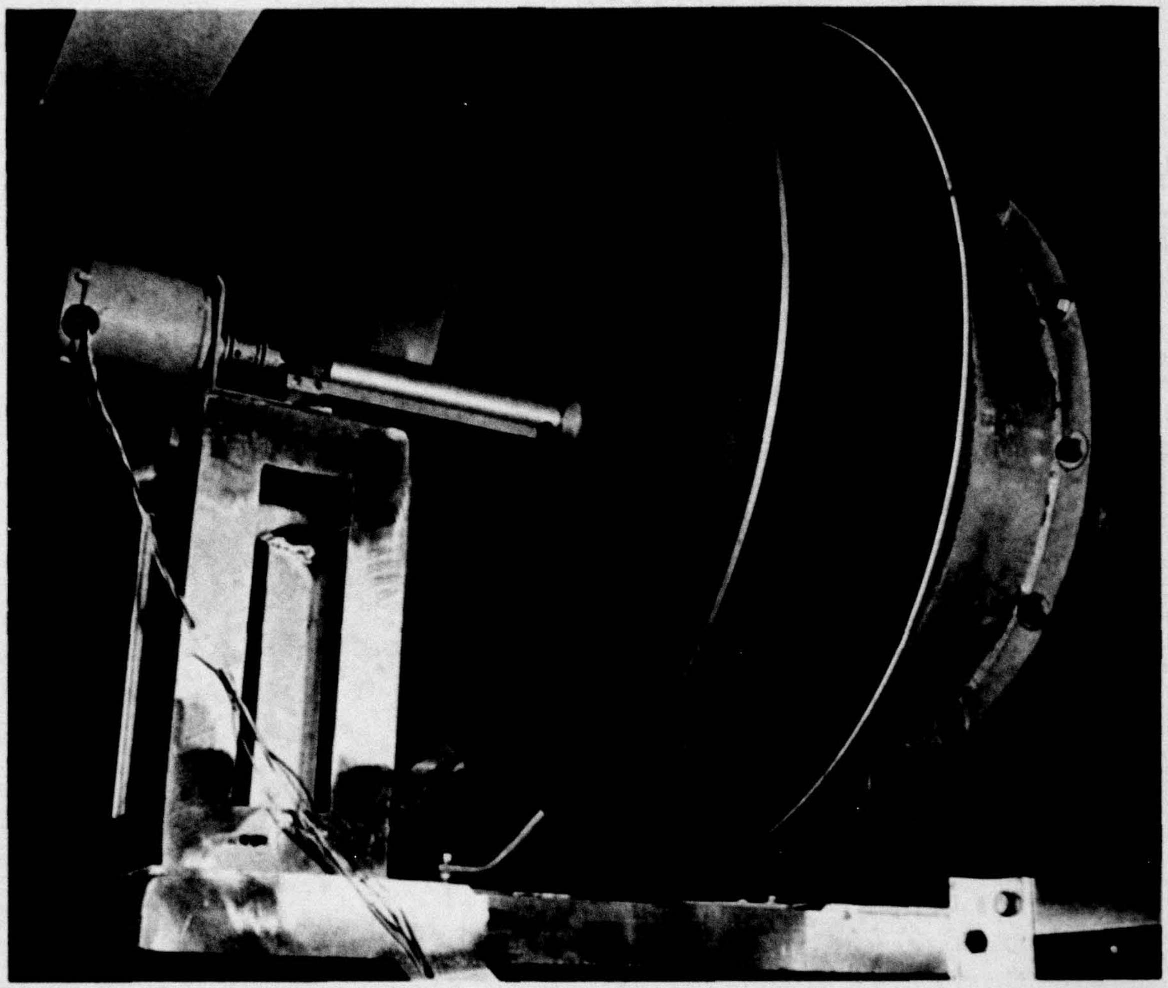

[redacted]

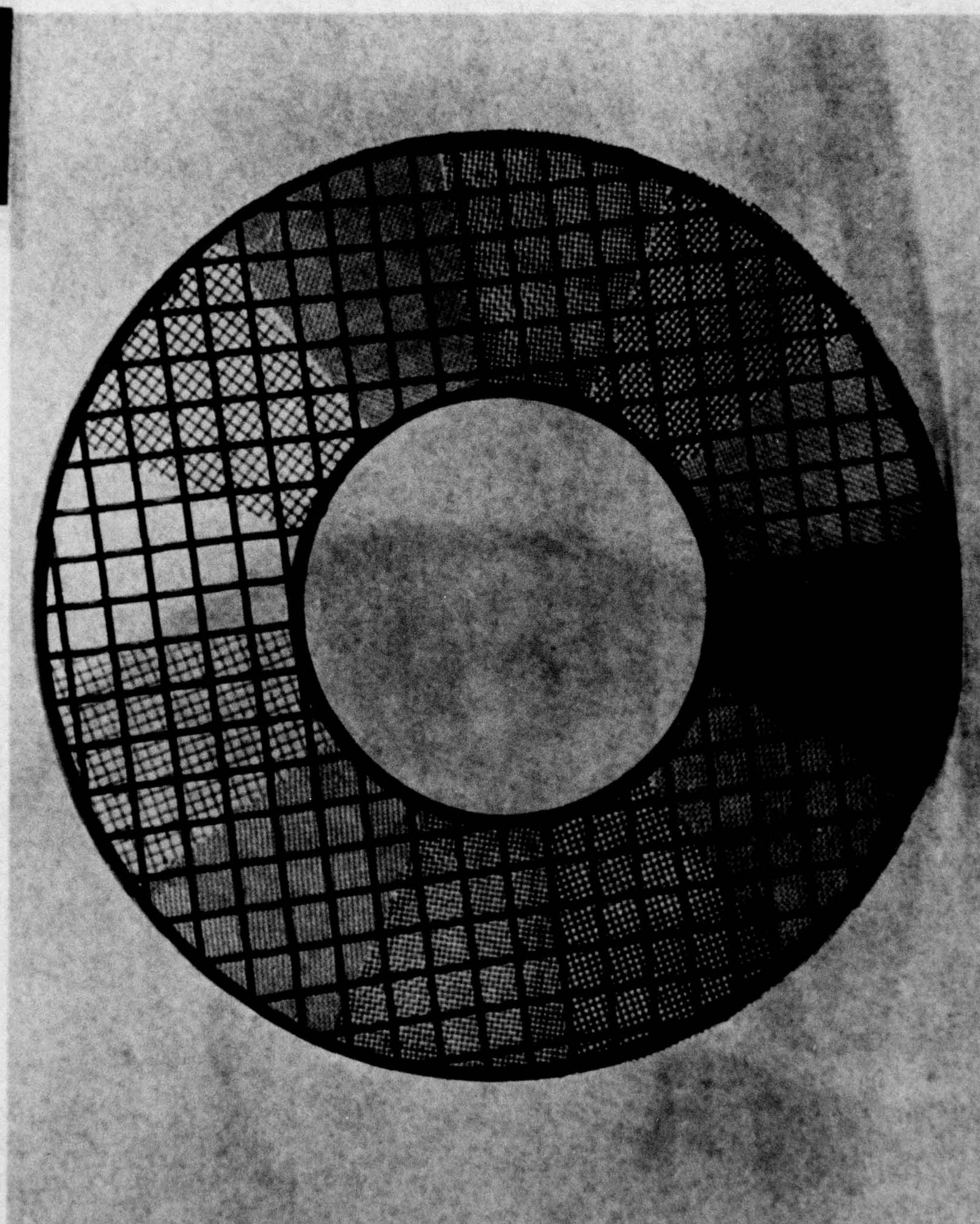

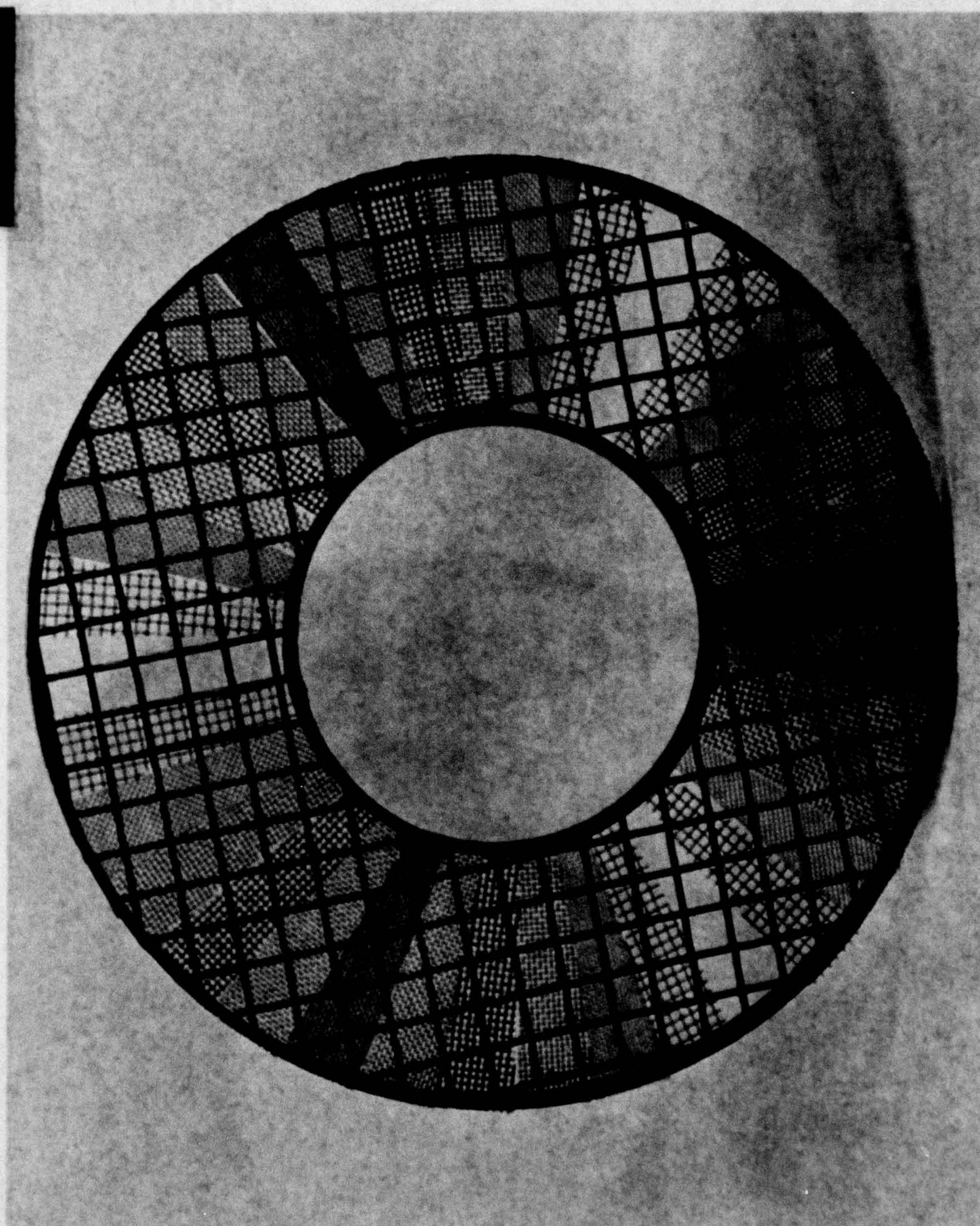

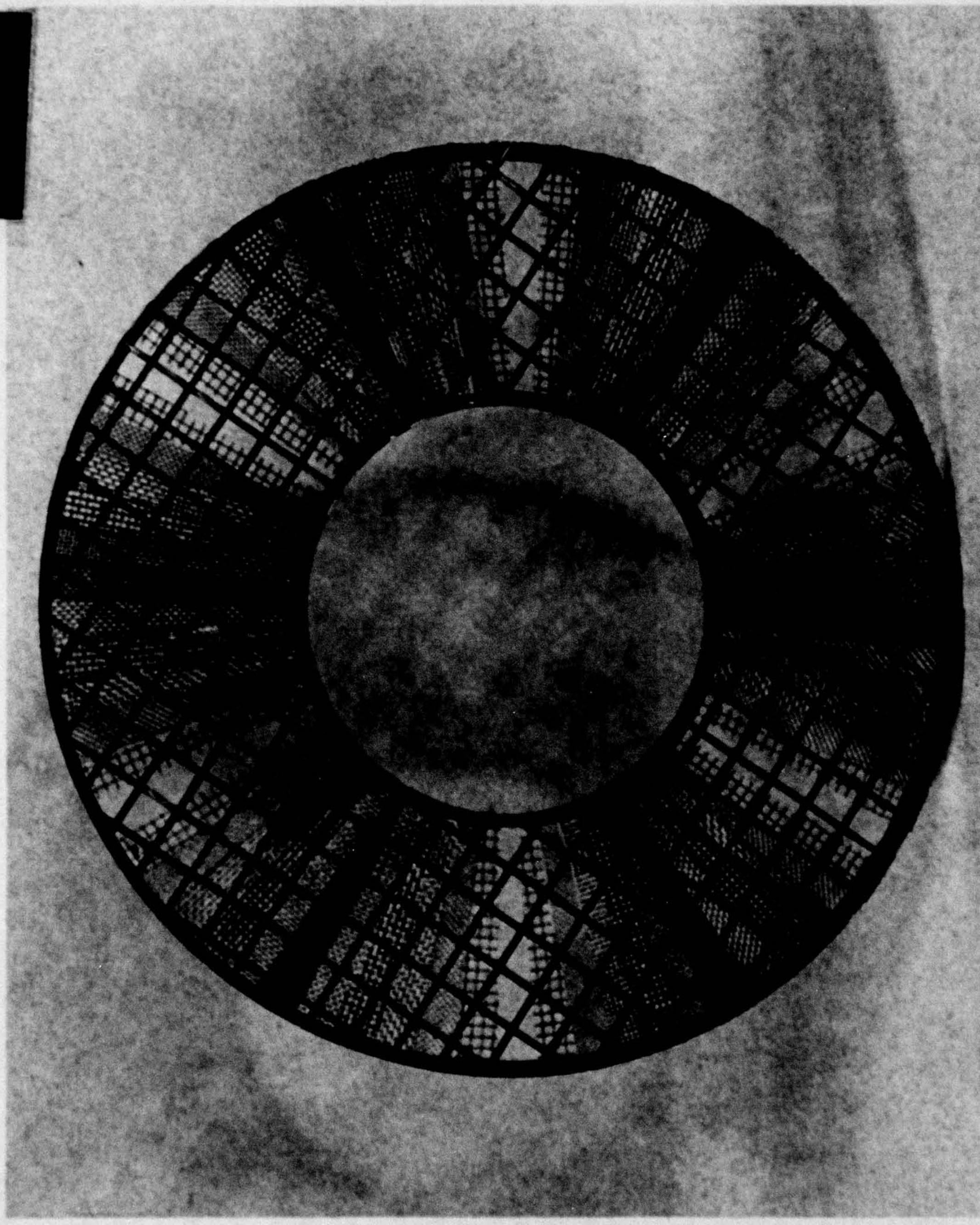

[redacted]

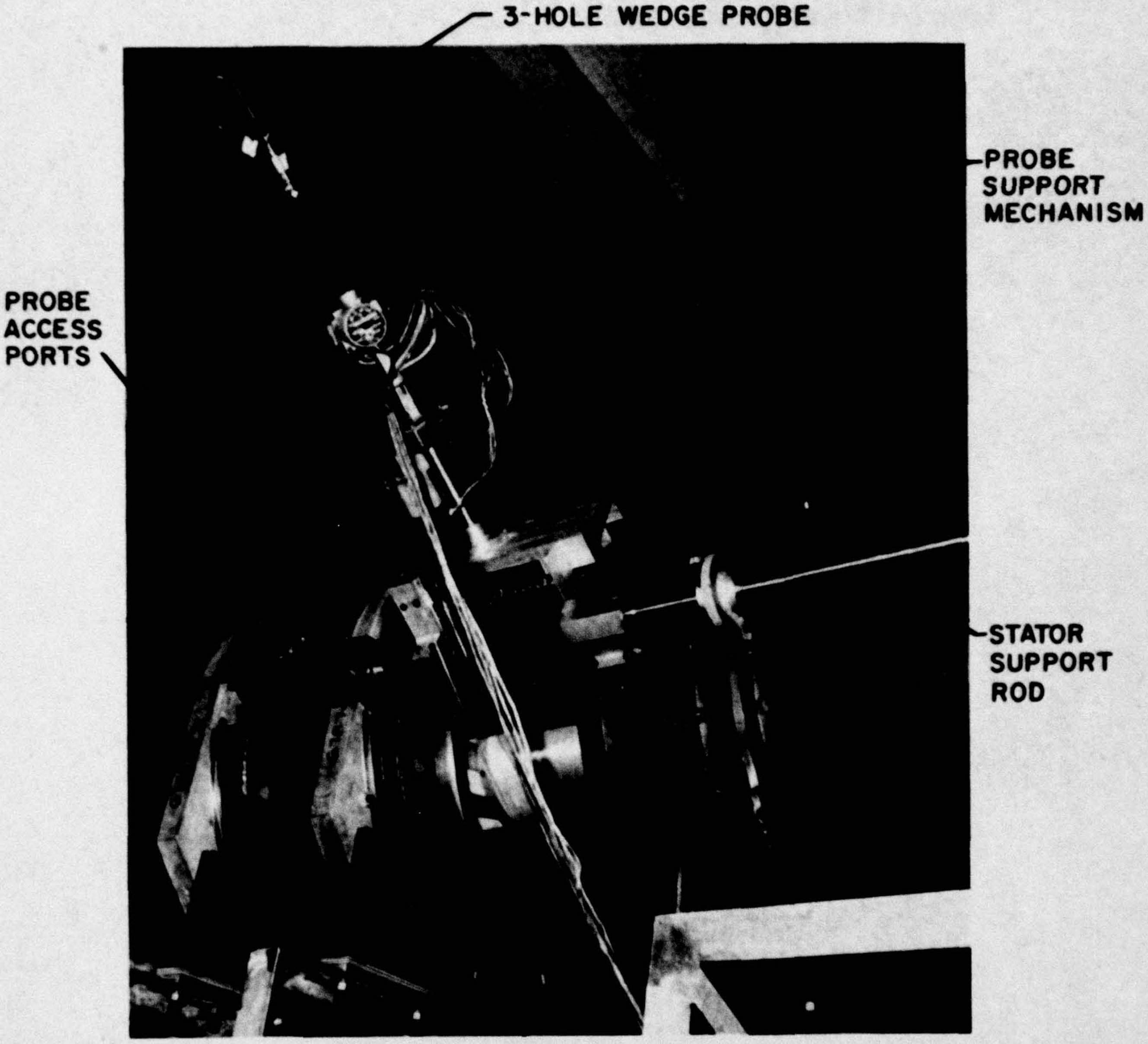

[redacted]

[redacted]

[redacted]

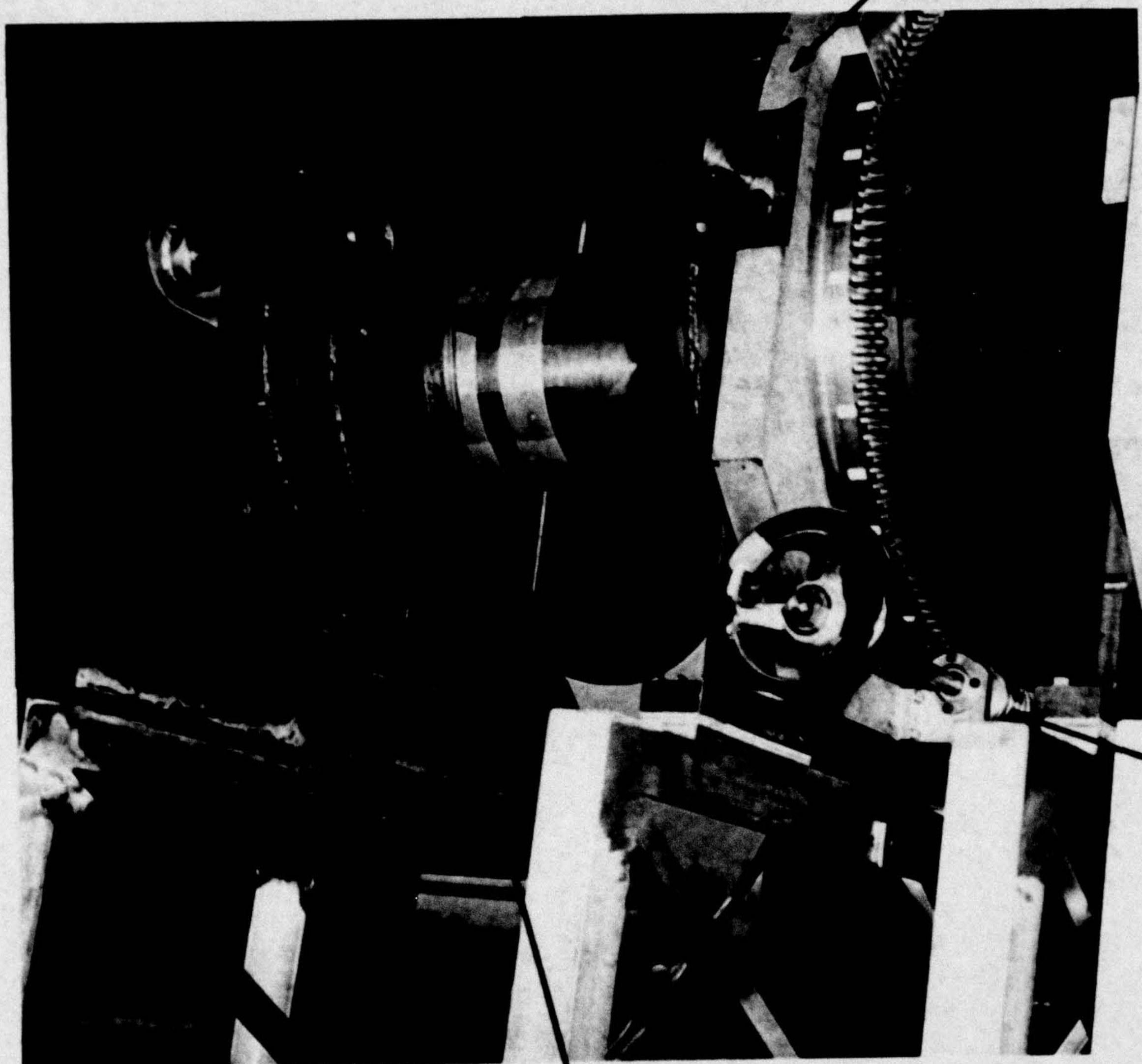

[redacted]

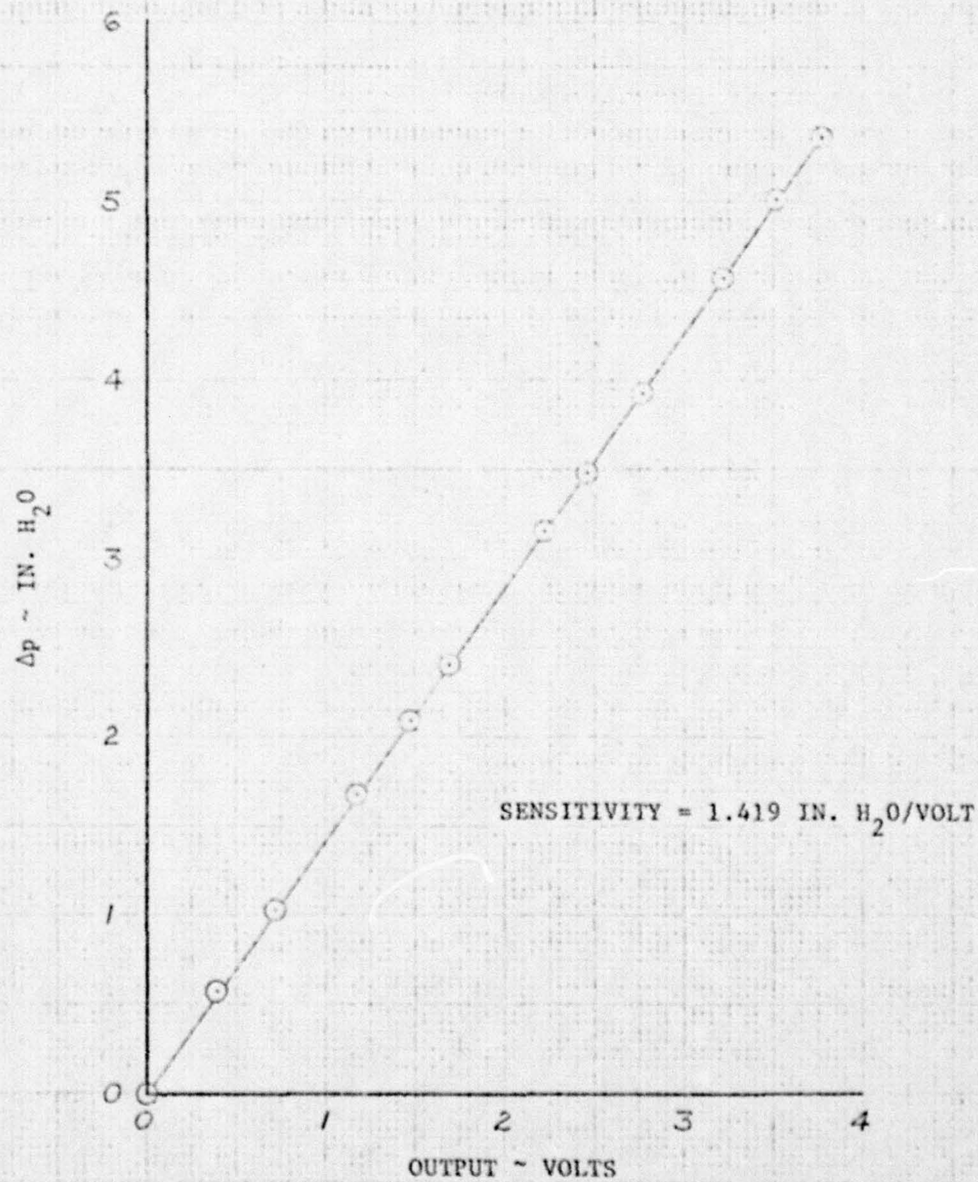

Figure 6. Typical Calibration Record for Validyne Engineering Corporation Model DP 15 0.5 PSID Variable Differential Pressure Transducer

June 22, 1972
EPB:mac

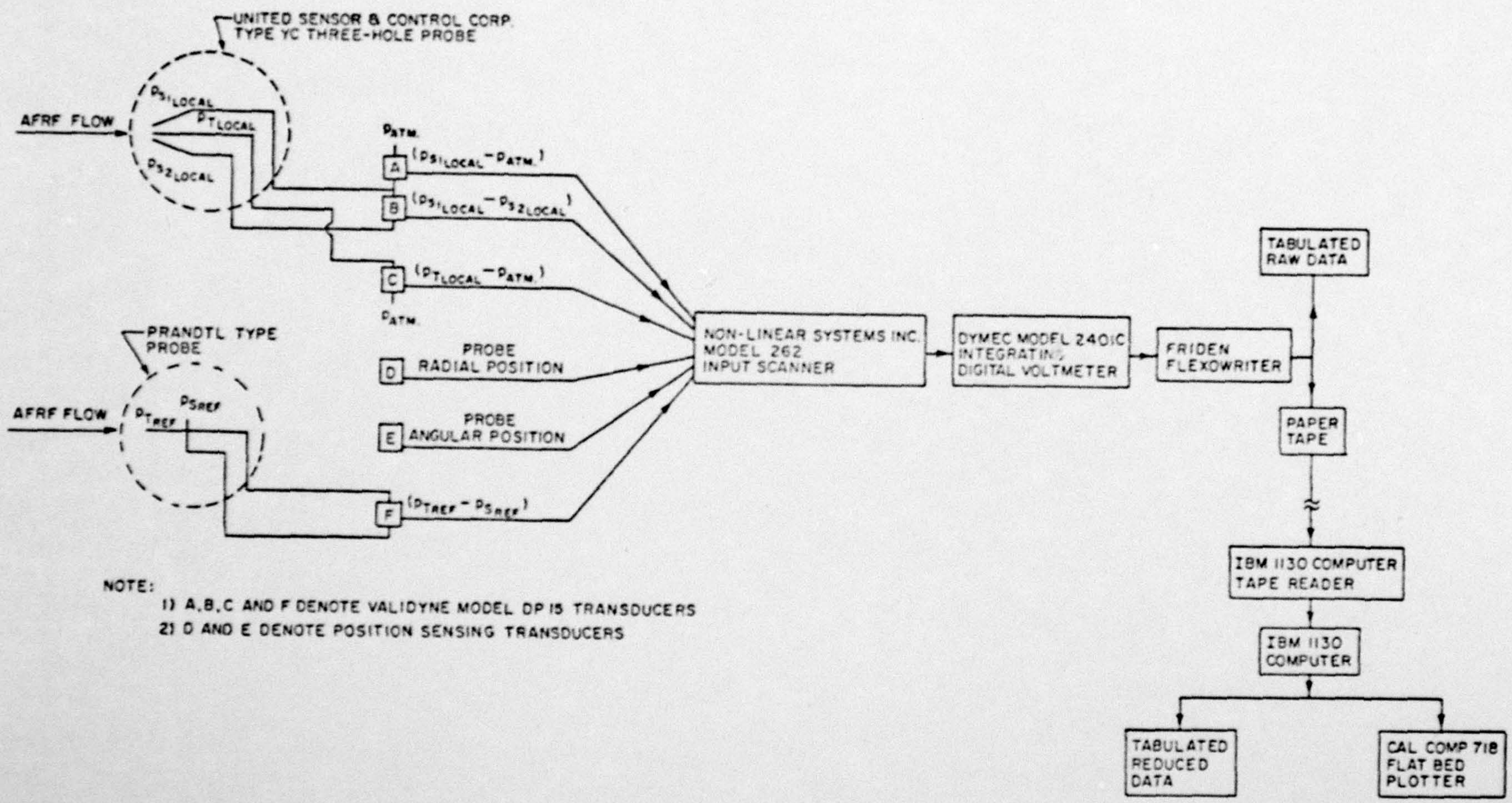

Figure 7. AFRF Shakedown Test Series Data Acquisition and Reduction System

Figure 8. ORL Axial Flow Research Fan Reference Velocity Vs. Throttle Position and Auxiliary Fan Inverter Frequency

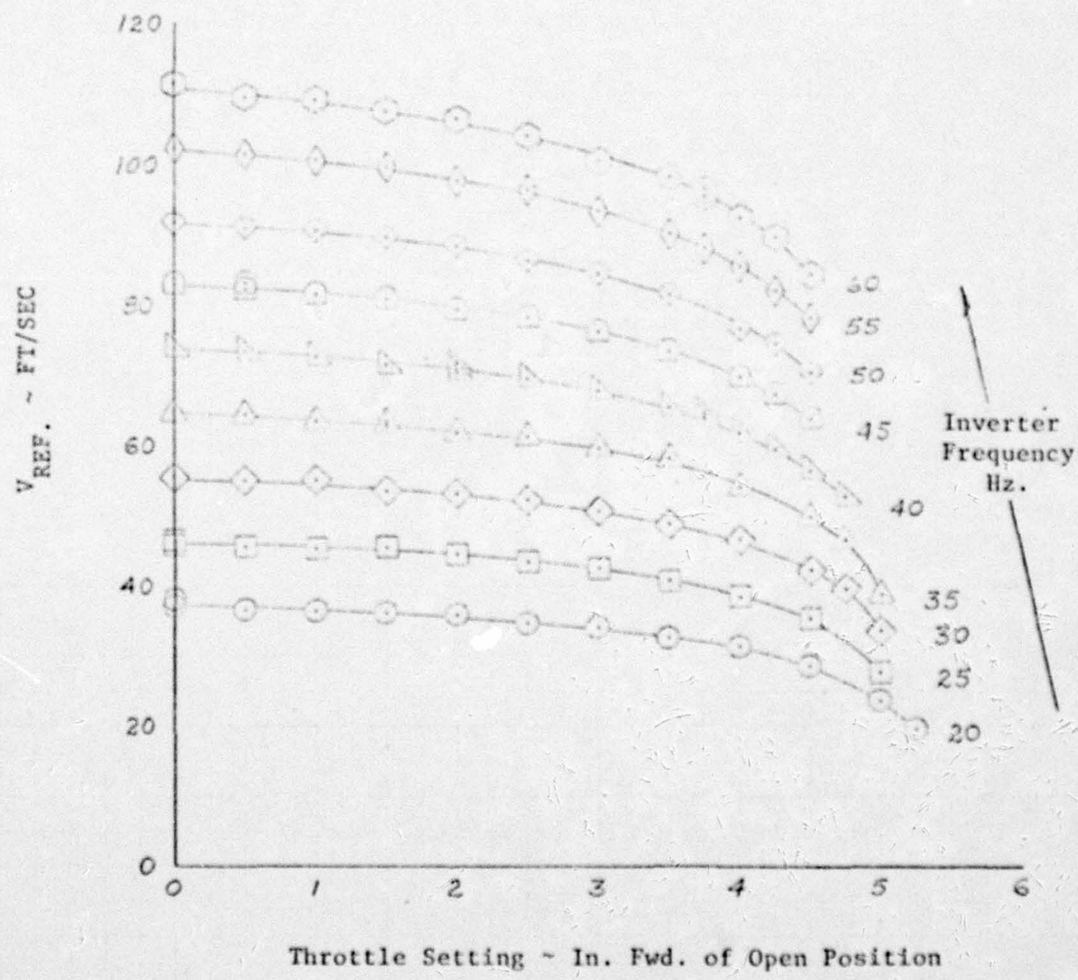

Figure 9. ORL Axial Flow Research Fan Static Pressure Distribution Vs. Throttle Position

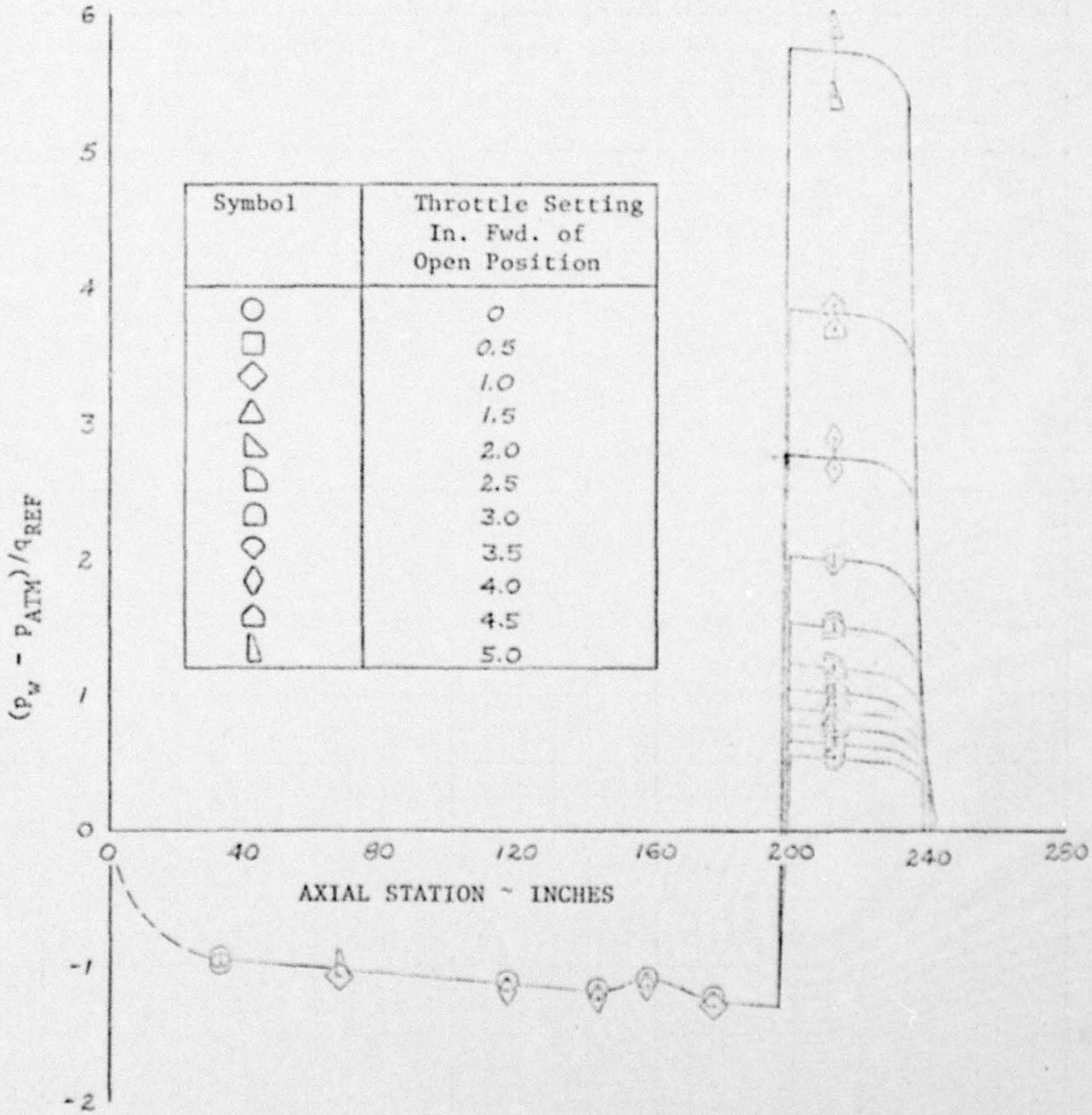

Figure 10. ORL Axial Flow Research Fan Back Pressure Vs. Throttle Position and Reference Velocity

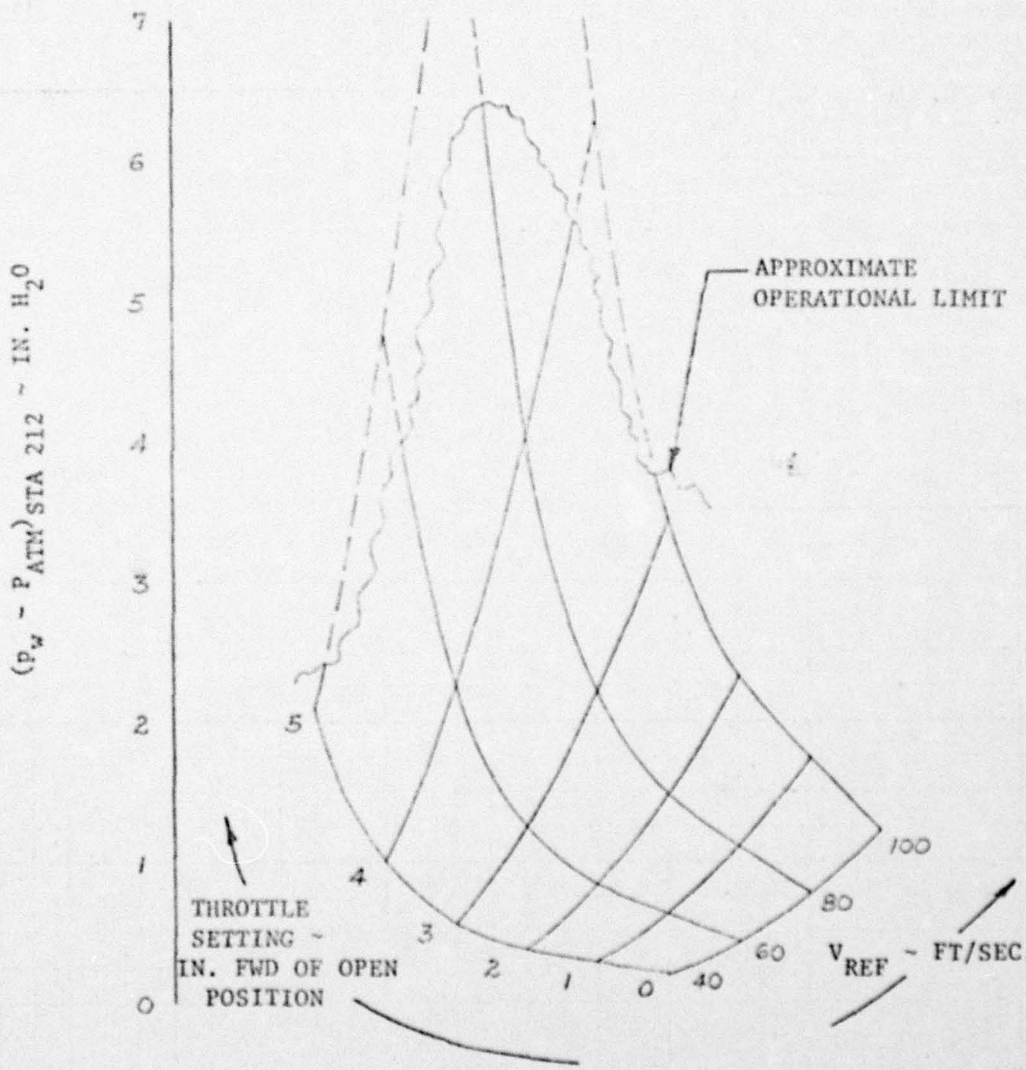

June 22, 1972
EPB:mac

Figure 11a. AFRF Shakedown Test No. 24 - Local Velocity vs Radius

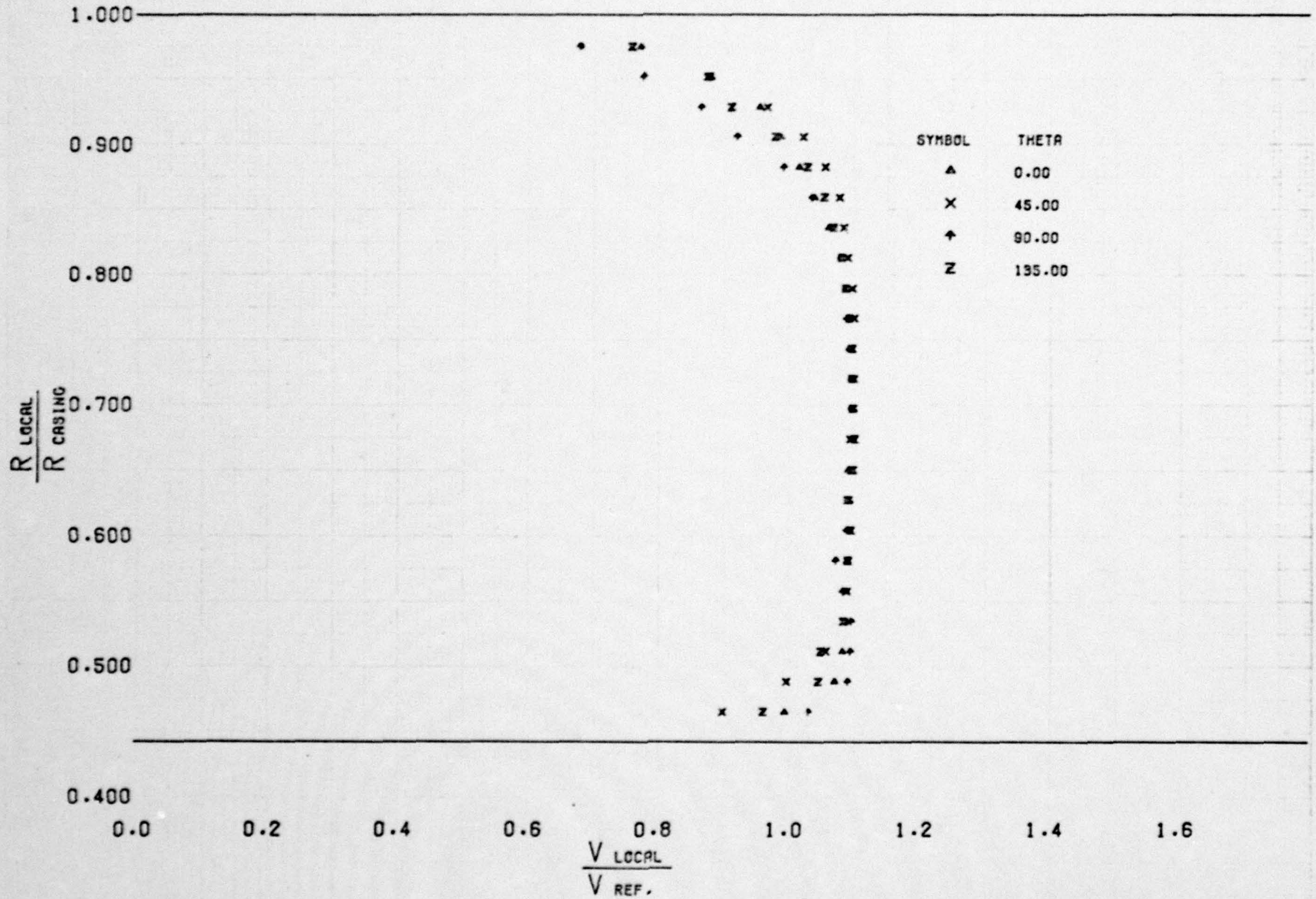

June 22, 1972
EPB:mac

Figure 11b. AFRF Shakedown Test No. 24 - Local Velocity vs Radius

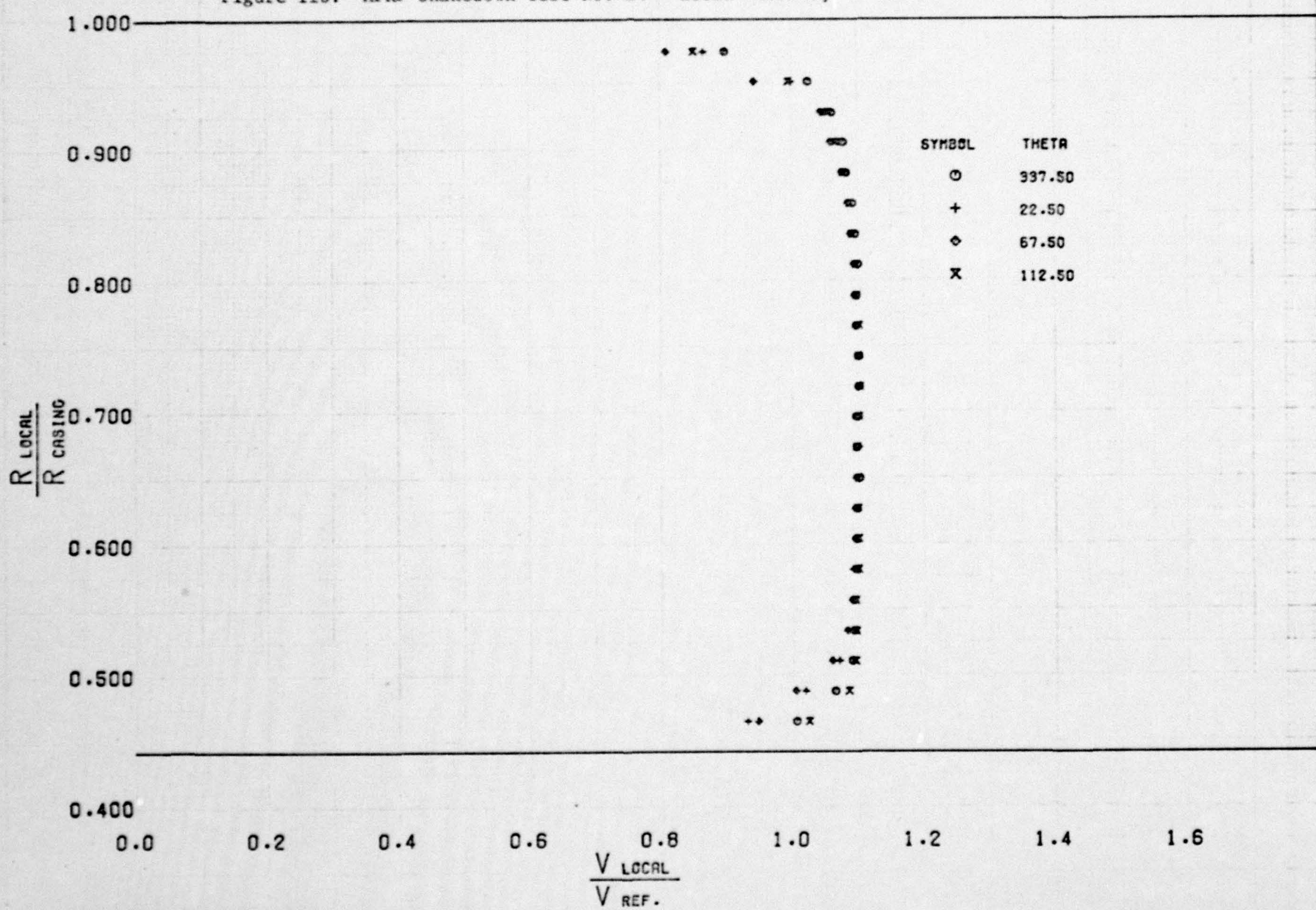

June 22, 1972
EPB:mac

Figure 11c. AFRF Shakedown Test No. 24 - Total Pressure vs Radius

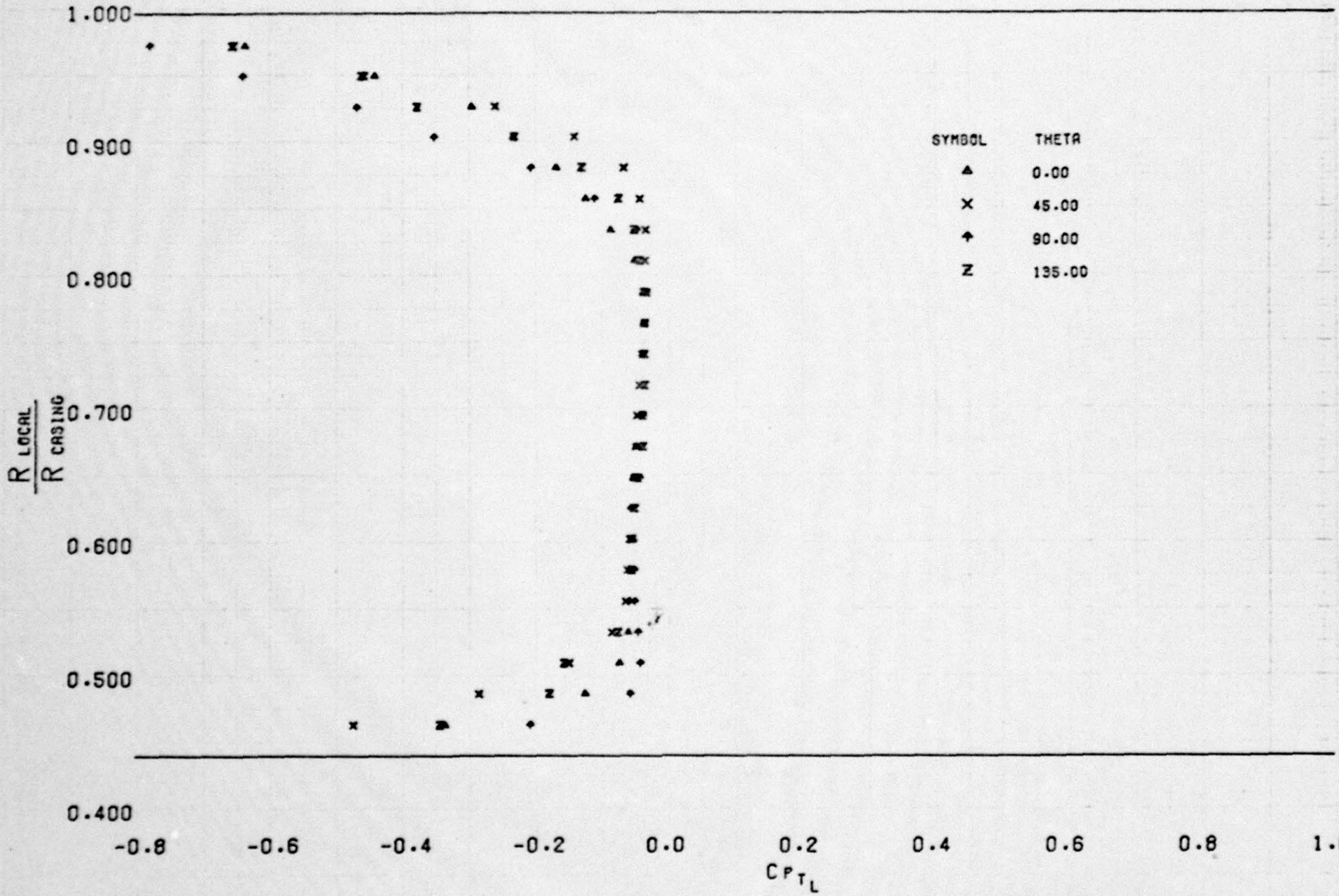

June 22, 1972
EPB:mac

Figure 11d. AFRF Shakedown Test No. 24 - Total Pressure vs. Radius

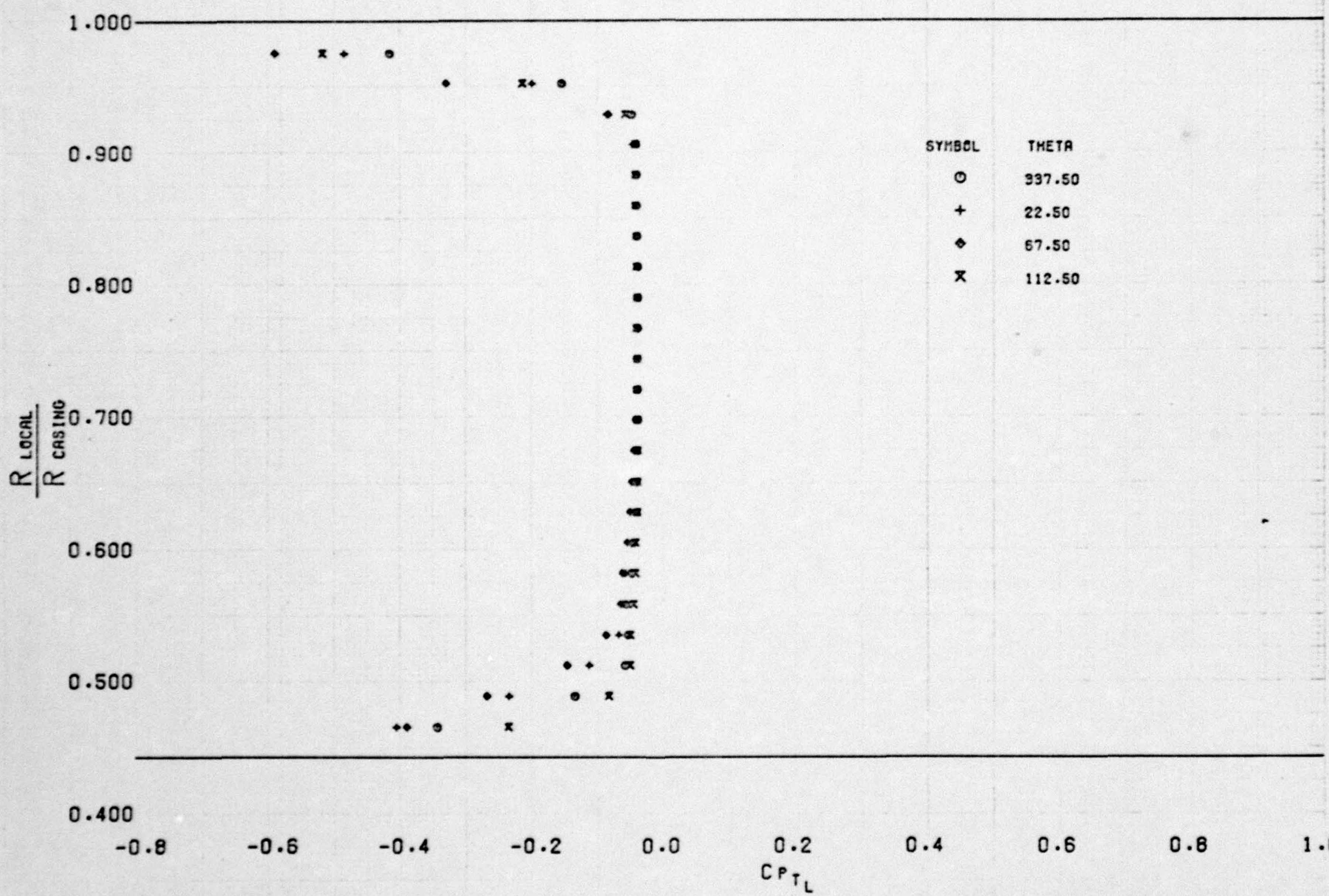

June 22, 1972
EPB:mac

Figure 11e. AFRF Shakedown Test No. 24 - Flow Angle vs. Radius

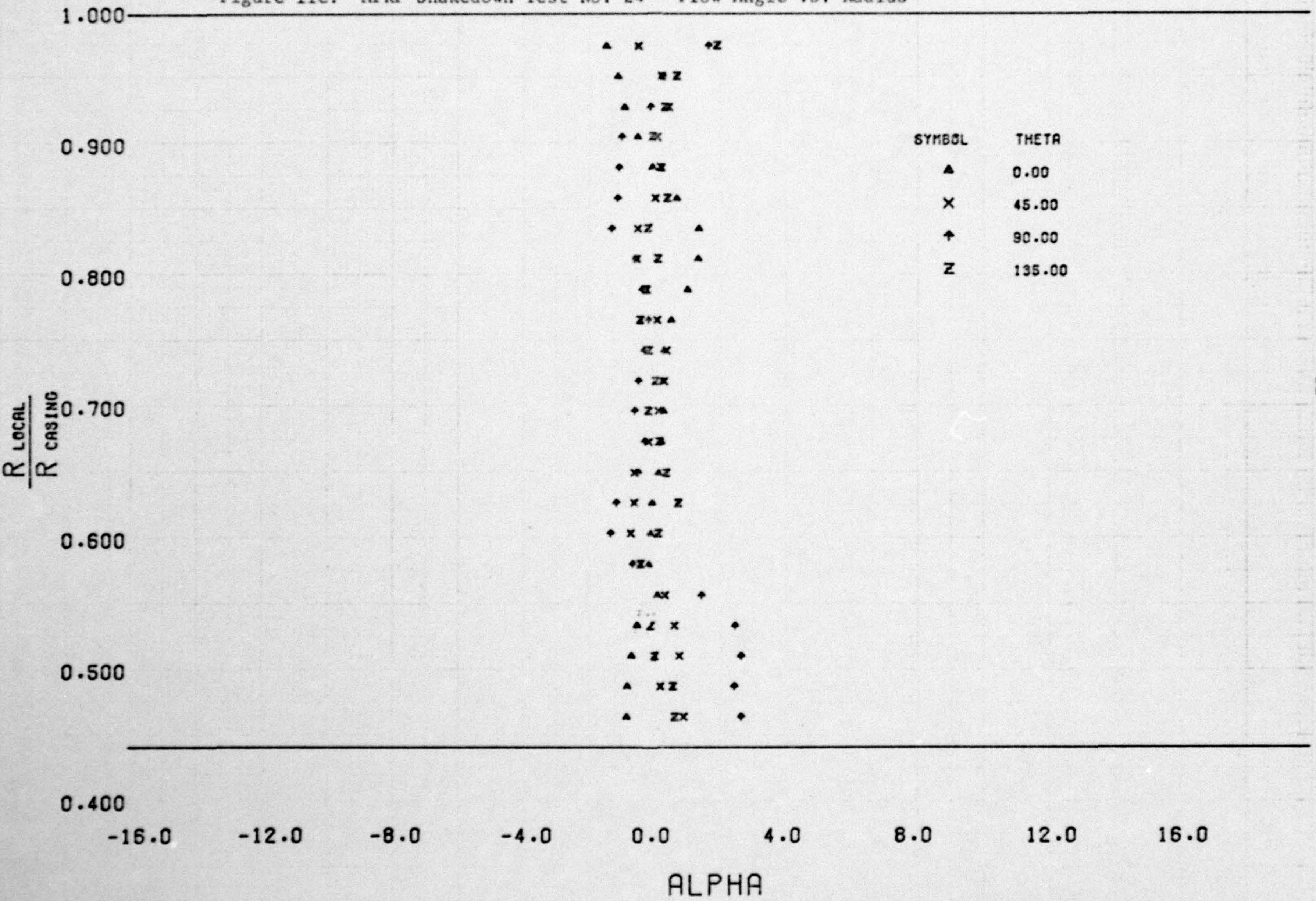

June 22, 1972
EPB:mac

Figure 11f. AFRF Shakedown Test No. 24 - Flow Angle vs. Radius

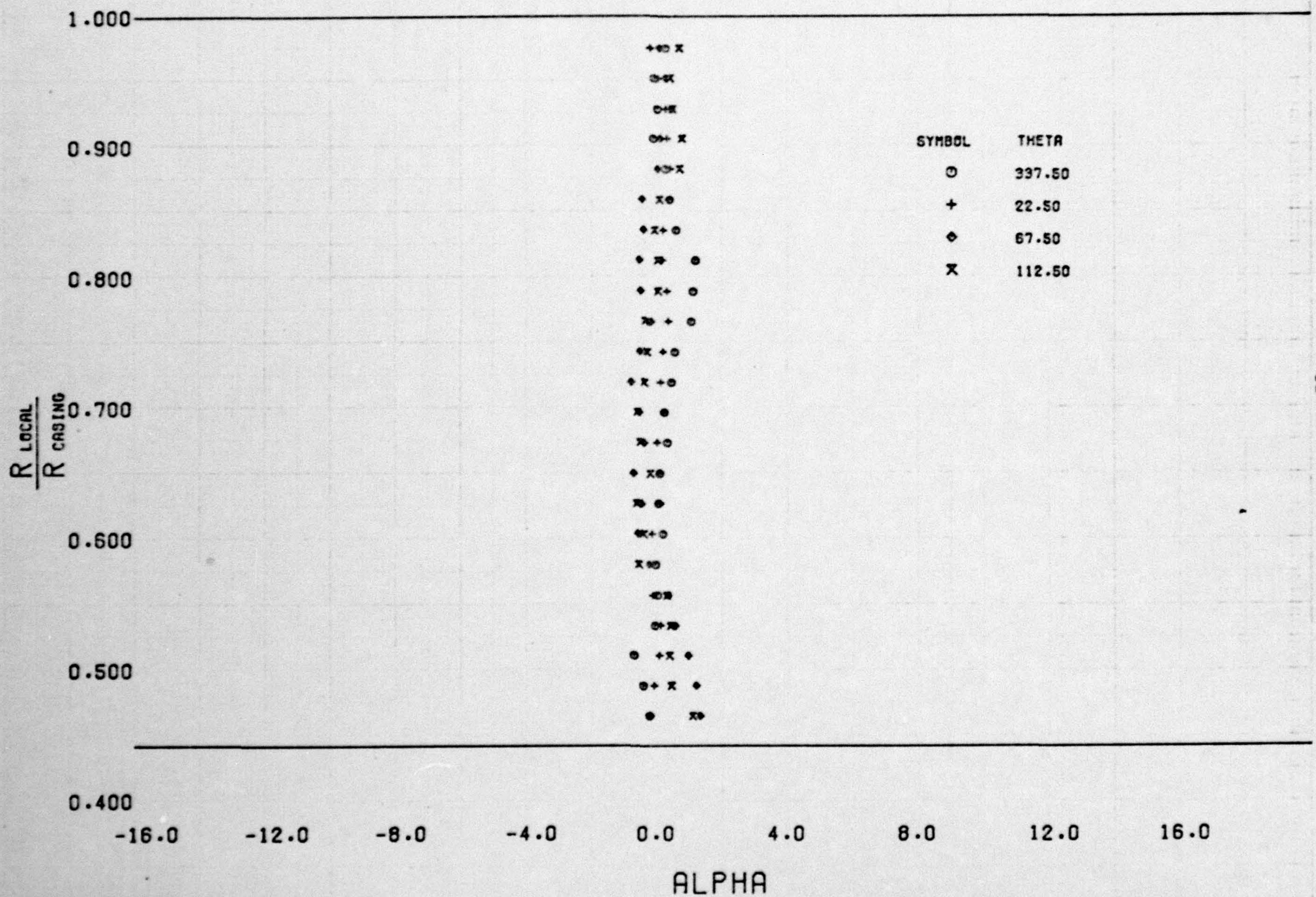

[redacted]

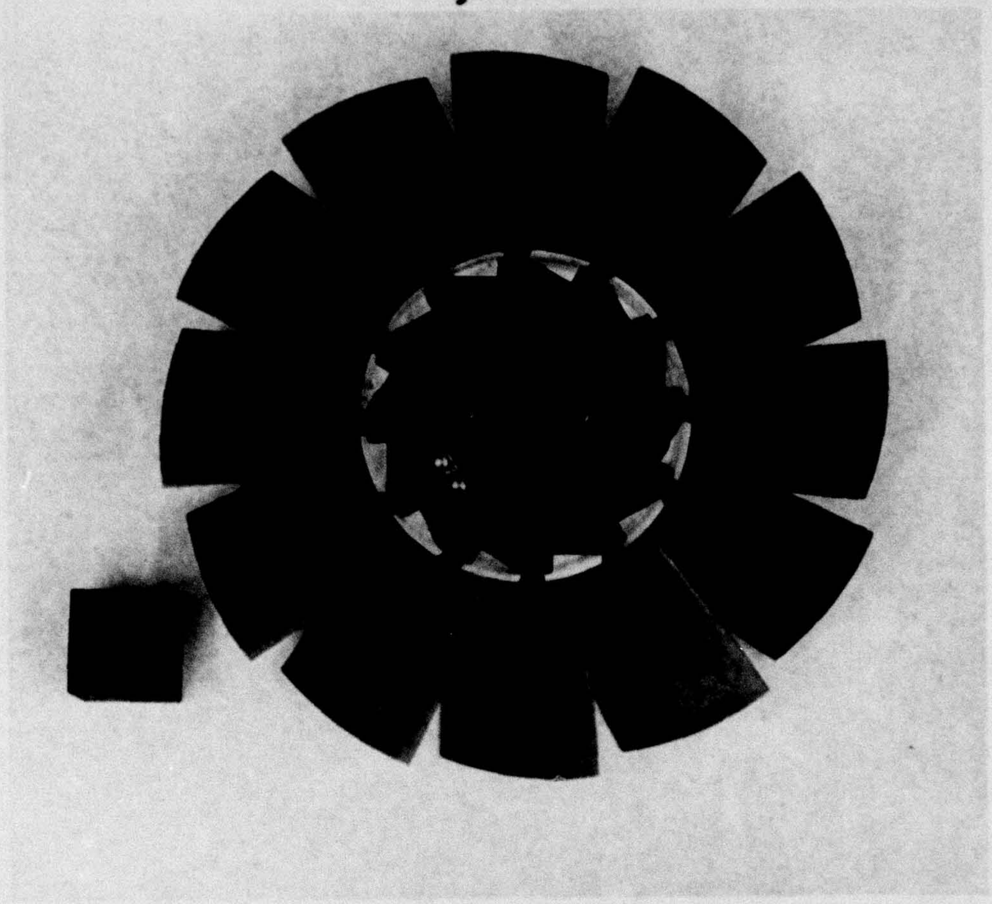

Figure 11. [illegible] Life Test Rotor With 12 Shims Installed.

June 22, 1972
EPB:mac

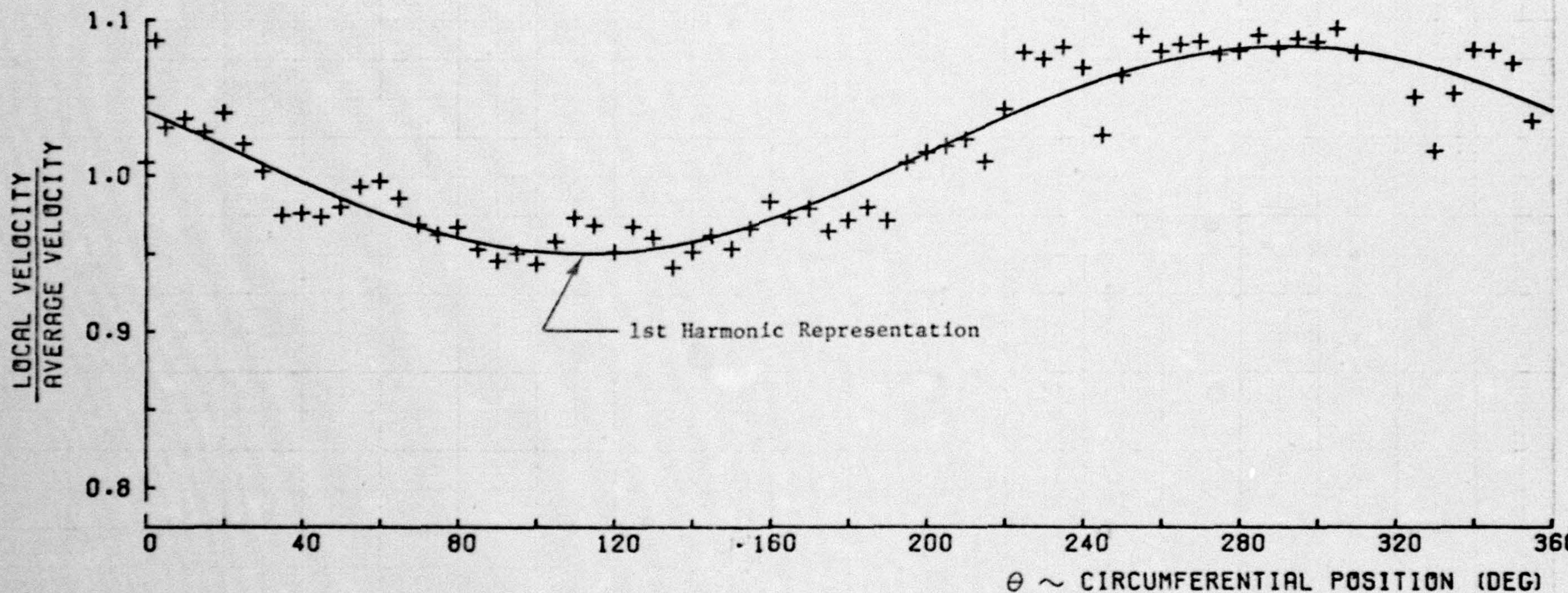

Figure 13a. Measured Circumferential Variation in Axial Velocity Ratio at the Rotor Inlet Due to the One-Cycle Disturbance Generating Screen

June 22, 1972
EPB:mac

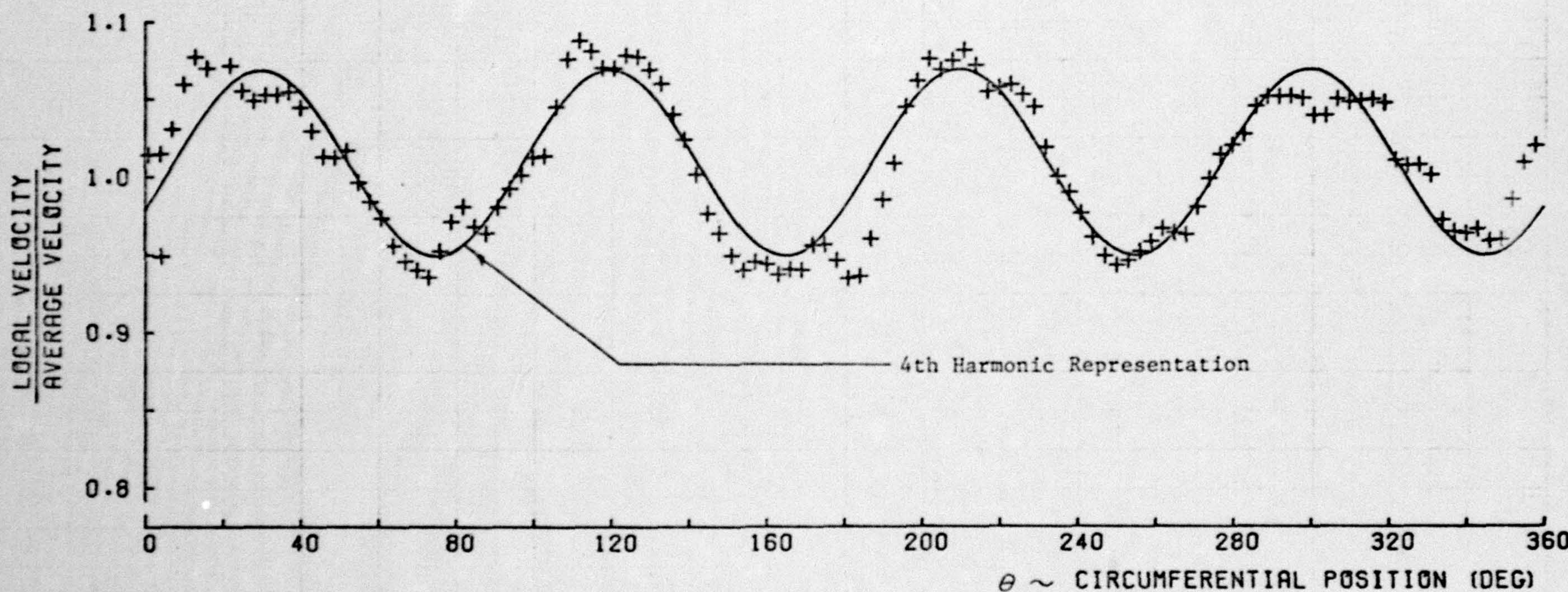

Figure 13b. Measured Circumferential Variation in Axial Velocity Ratio at the Rotor Inlet Due to the Four-Cycle Disturbance Generating Screen

June 22, 1972
EPB:mac

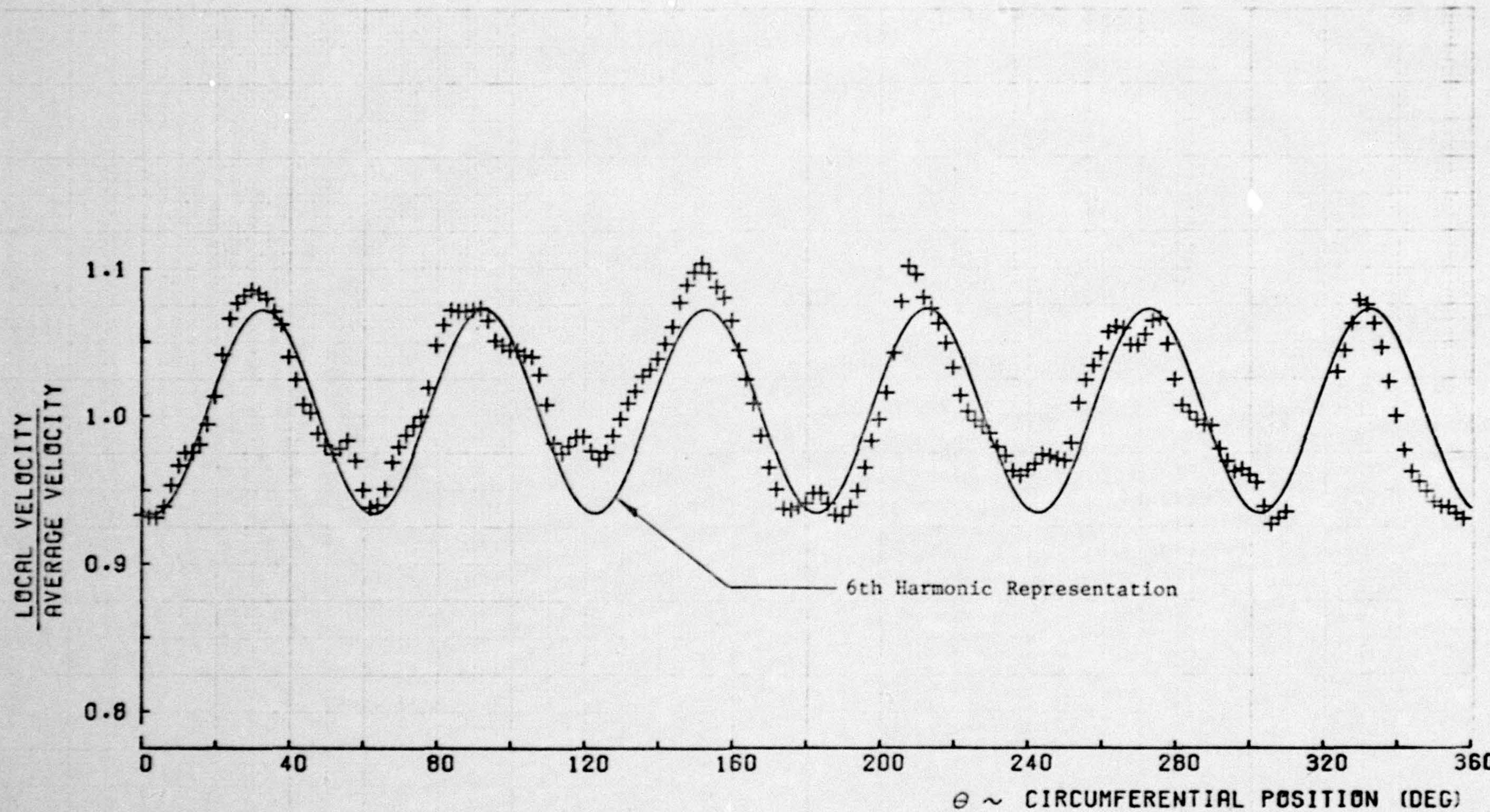

Figure 13c. Measured Circumferential Variation in Axial Velocity Ratio at the Rotor Inlet Due to the Six-Cycle Disturbance Generating Screen

Figure 14. Variation of Reduced Frequency at Zero Mean Incidence With Number of Disturbance Cycles per Revolution and Stagger Angle

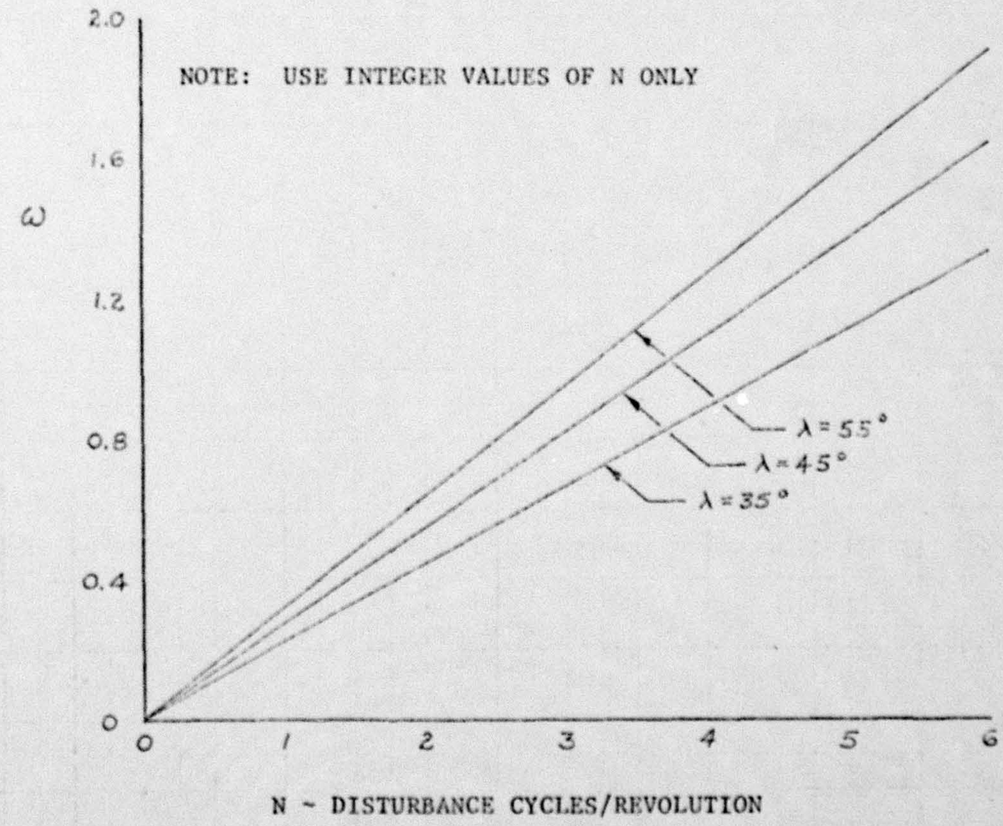

June 22, 1972
EPB:mac

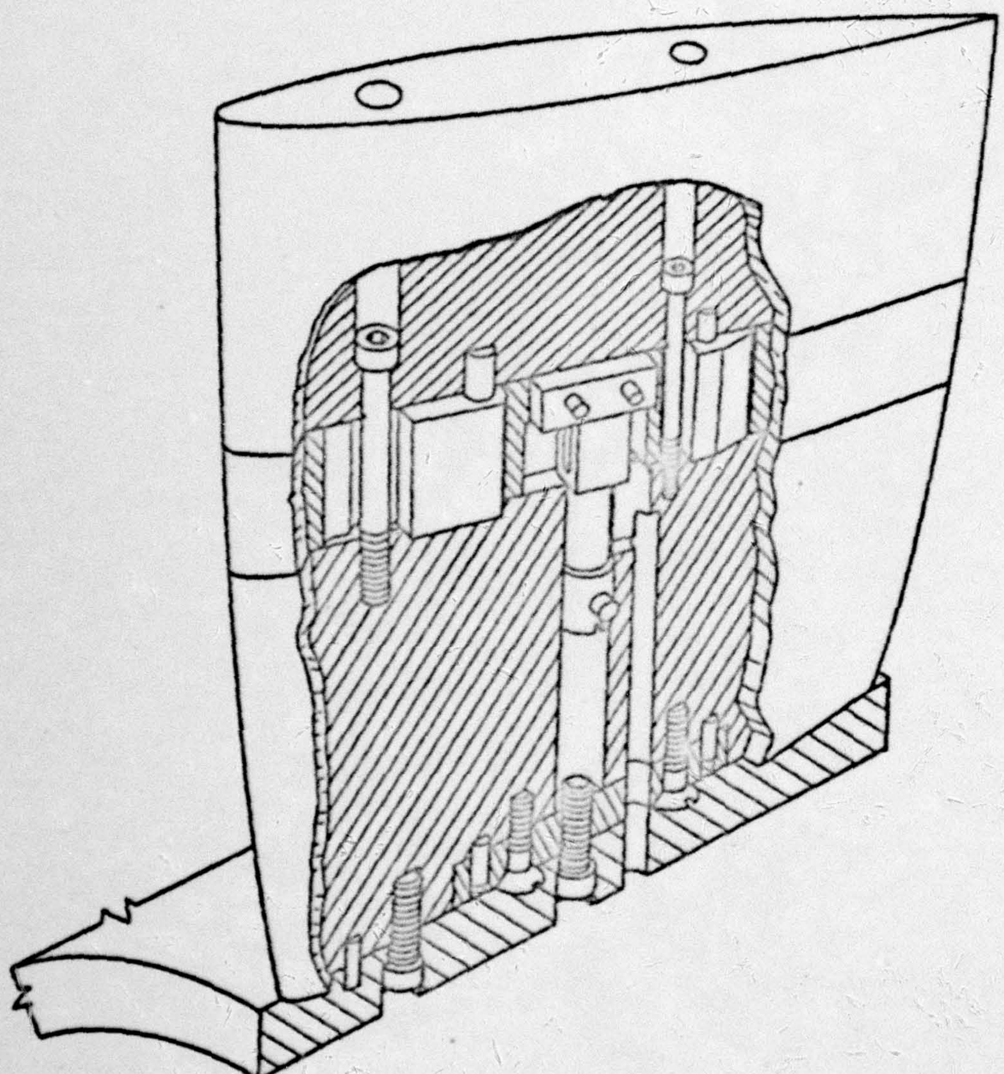

Figure 15. Schematic of Strain Gage Sensor Installation for ORL Axial Flow Research Fan Rotor Blade Section

June 22, 1972
EPB:mac

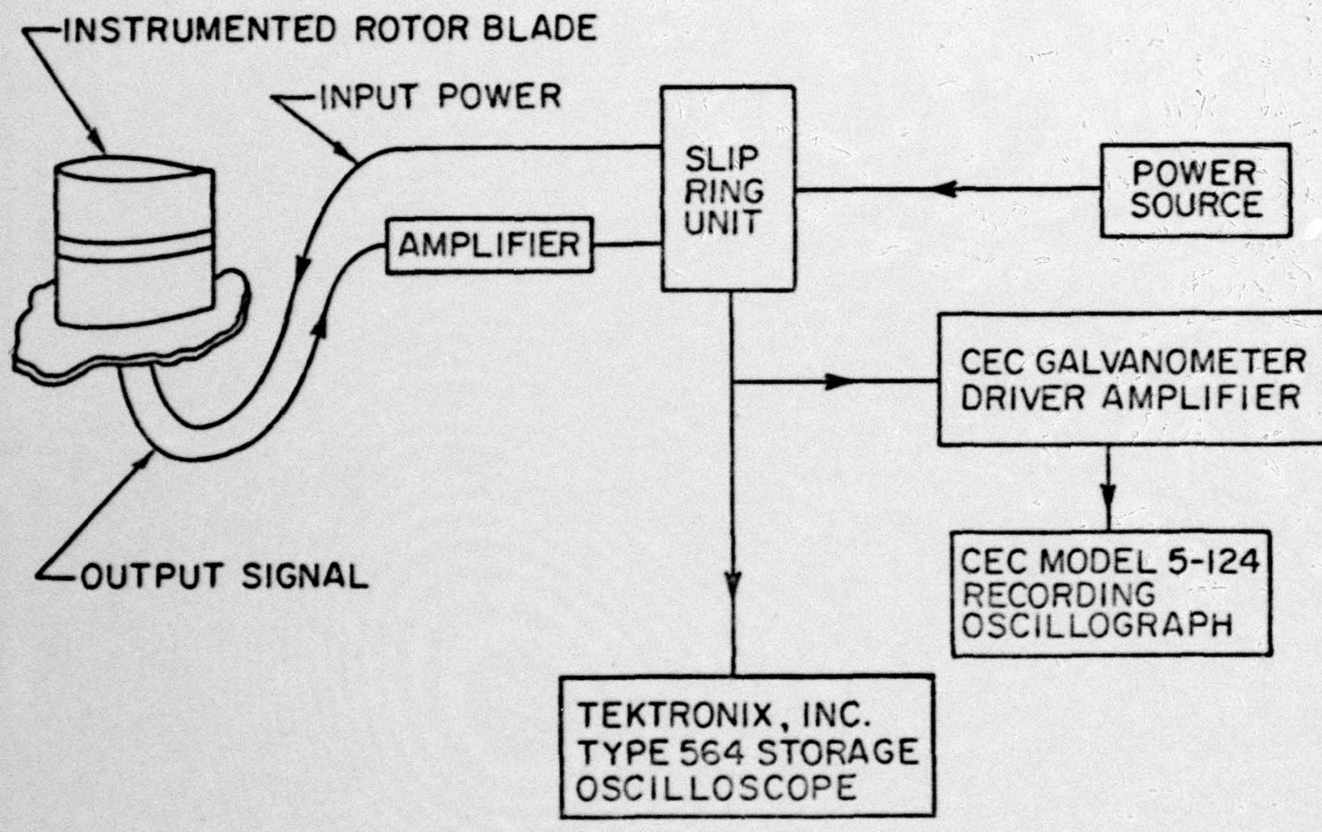

Figure 16. Instrumentation Schematic for AFRF Tests with a Rotating Blade

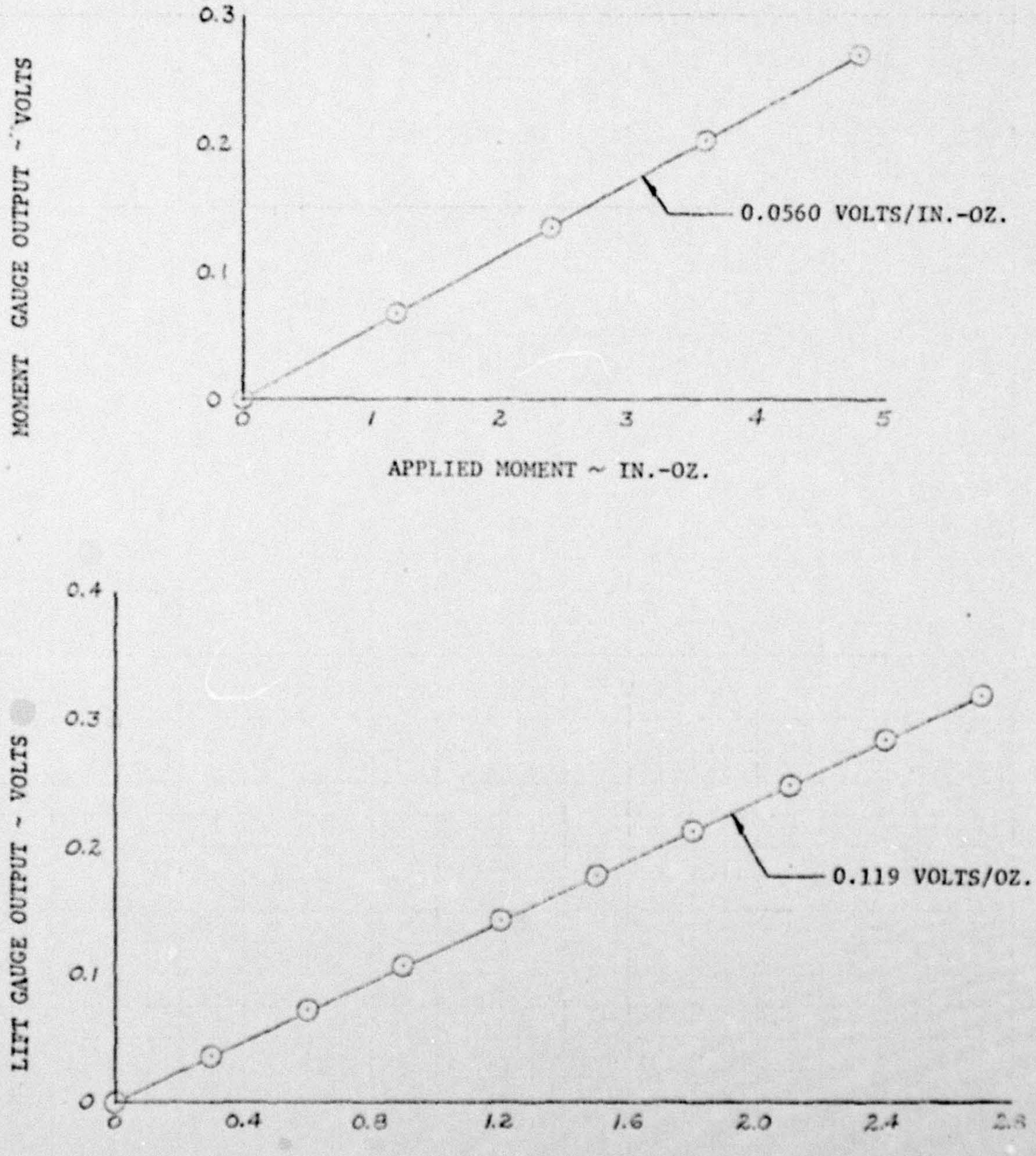

Figure 17. Results of Static Calibration of AFRF Instrumented Blade Sensor

June 22, 1972
EPB:mac

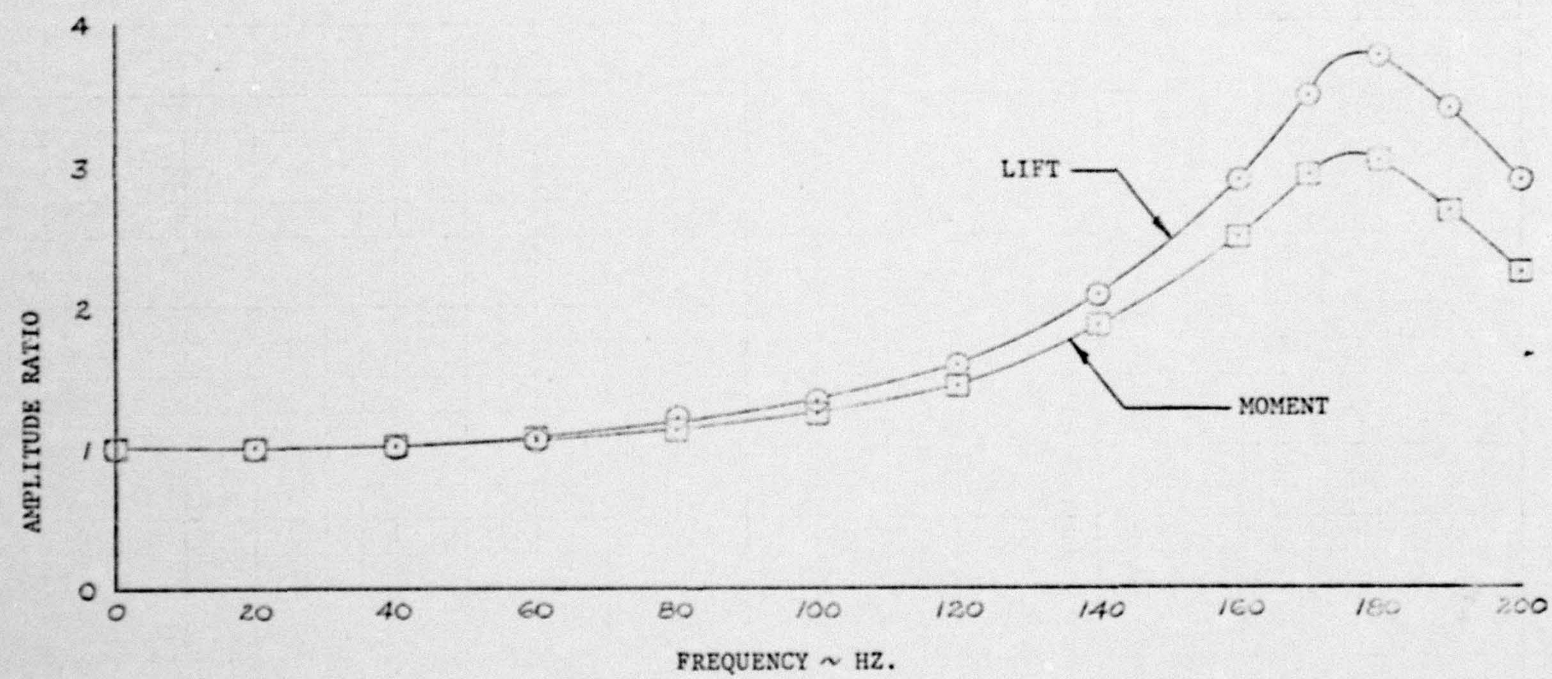

Figure 18. Results of Dynamic Calibration of AFRF Instrumented Blade Sensor

DISTRIBUTION LIST FOR UNCL TM 72-109

Commander
Naval Ordnance Systems Command
Department of the Navy
Washington, D. C. 20360
Attn: Library
Code ORD-632
(Copies 1 and 2)

Naval Ordnance Systems Command
Attn: S. R. Marcus
Code ORD-03A
(Copy No. 3)

Naval Ordnance Systems Command
Attn: Code ORD-034B
(Copy No. 4)

Naval Ordnance Systems Command
Attn: T. E. Peirce
Code ORD-035B
(Copy No. 5)

Naval Ordnance Systems Command
Attn: G. R. Moltrup
Code ORD-54
(Copy No. 6)

Naval Ordnance Systems Command
Attn: O. Seidman
Code ORD-035
(Copy No. 7)

Naval Ordnance Systems Command
Attn: Chief Technical Analyst
Code ORD-05121
(Copy No. 8)

Naval Ordnance Systems Command
Attn: Chief Analyst, J. J. Bellaschi
Code ORD-03B
(Copy No. 9)

Commander
Naval Ship Systems Command
Department of the Navy
Washington, D. C. 20360
Attn: A. R. Paladino
DIV 037
(Copy No. 10)

Naval Ship Systems Command
Attn: R. Sherwood
DIV 037
(Copy No. 11)

Naval Ship Systems Command
Attn: Library
Code 2052
(Copy No. 12)

Commander
Naval Ship Engineering Center
Department of the Navy
Washington, D. C. 20360
Attn: W. L. Louis
Code 6136B
(Copy No. 13)

Naval Ship Engineering Center
Attn: R. M. Petros
Code 6148
(Copy No. 14)

Commanding Officer
Naval Underwater Systems Center
Newport, Rhode Island 02840
Attn: J. F. Brady
(Copy No. 15)

Officer-in-Charge
Naval Undersea Research &
Development Center
Pasadena Laboratory
3202 E. Foothill Boulevard
Pasadena, California 91107
Attn: J. W. Hoyt
(Copy No. 16)

Naval Undersea Research &
Development Center
Attn: J. Green
(Copy No. 17)

Naval Undersea Research &
Development Center
San Diego Laboratory
San Diego, California 92132
Attn: A. G. Fabula
Code 6005
(Copy No. 18)

DISTRIBUTION LIST FOR UNCL TM 72-109 (Cont'd)

Commander
Naval Ordnance Laboratory
Silver Spring, Maryland 20910
Attn: R. B. Knowles
(Copy No. 19)

Naval Ordnance Laboratory
Attn: Library
(Copy No. 20)

Commanding Officer & Director
Naval Ship Res. & Dev. Center
Department of the Navy
Bethesda, Maryland 20034
Attn: W. Morgan
Code 526
(Copy No. 21)

Naval Ship Res. & Dev. Center
Attn: M. Strasberg
Code 901
(Copy No. 22)

Naval Ship Res. & Dev. Center
Attn: J. B. Hadler
Code 520
(Copy No. 23)

Naval Ship Res. & Dev. Center
Attn: M. Sevik
Code 019
(Copy No. 24)

Dr. A. H. Stenning
Department of Mechanical Engineering
Lehigh University
Bethlehem, Pennsylvania 18001
(Copy No. 25)

Von Karman Inst. for Fluid Dynamics
Turbomachinery Laboratory
Rhode-Saint-Genese
BELGIUM
Attn: Library
(Copy No. 26)

Dr. W. R. Sears
Graduate School of Aerospace Eng.
Cornell University
Grumman Hall
Ithaca, New York 14850
(Copy No. 27)

Mr. W. Whippen
Allis-Chalmers
Box 712
York, Pennsylvania 17405
(Copy No. 28)

Dr. Hsuan Yeh, Director
Towne School of Civil & Mech. Eng.
University of Pennsylvania
Room 113 Towne
220 S. 33rd Street
Philadelphia, Pennsylvania 19104
(Copy No. 29)

Dr. Frank Carta
Supervisor, Aeroelastics
United Aircraft Corp., Res. Lab.
400 Main Street
E. Hartford, Connecticut 06108
(Copy No. 30)

Dr. G. K. Serovy
Professor
Mechanical Engineering Dept.
Iowa State University
Ames, Iowa 50010
(Copy No. 31)

U. S. Naval Post Graduate School
Monterey, California
Attn: Library
(Copy No. 32)

Wright Patterson Air Force Base
Dayton, Ohio 45433
Attn: Dr. William H. Heiser
(Copy No. 33)

Wright-Patterson Air Force Base
Attn: Mr. E. C. Simpson, AFAPL/TB
(Copy No. 34)

DISTRIBUTION LIST FOR UNCL TM 72-109 (Cont'd)

Dr. Robert Goulard
Director
Project Squid
Purdue University
Jet Propulsion Center
W. Lafayette, Indiana 47907
(Copy No. 35)

Dr. A. J. Acosta
Professor of Mechanical Engineering
Division of Engineering &
Applied Science
California Institute of Technology
Pasadean, California 91109
(Copy No. 36)

Dr. R. A. Schmidtke
United Aircraft Coproration
Pratt & Whitney Aircraft Division
Box 2691
West Palm Beach, Florida 33402
(Copy No. 37)

Mr. W. R. Britsch
NASA Lewis Research Center
21000 Brookpark Road
Cleveland, Ohio 44135
(Copy No. 38)

Northern Research & Eng. Corporation
219 Vassar Street
Cambridge, Massachusetts 02139
Attn: Library
(Copy No. 39)

Dr. C. L. Morfey
Lecturer in Noise Research
University of Southampton
ISVR
Southampton, ENGLAND
(Copy No. 40)

Mr. Linwood C. Wright
Chief of Aerodynamics
AiResearch Mfg. Co.
2525 W. 190th Street
Torrance, California 90509
(Copy No. 41)

Dr. R. C. Dean, Jr., President
Creare, Inc.
Box 226
Hanover, New Hampshire 03755
(Copy No. 42)

Professor H. Marsh
Durham University
Durham, ENGLAND
(Copy No. 43)

Dr. L. H. Smith
Compressor & Fan Design Tech. Oper.
DTO, Mail Drop H-43
Cincinnati, Ohio 45215
(Copy No. 44)

Dr. D. H. Norrie
Department of Mech. Eng.
The University of Calgary
Alberta, Canada
(Copy No. 45)

SRC Turbomachinery Laboratory
Madingley Road
Cambridge
ENGLAND
Attn: Prof. J. H. Horlock
(Copy No. 46)

SRC Turbomachinery Laboratory
Attn: Library
(Copy No. 47)

Hydronautics, Inc.
Pindell School Road
Laurel, Maryland 20810
Attn: Library
(Copy No. 48)

Bell Aerospace
P. O. Box 1
Buffalo, New York 14240
Attn: Dr. W. Morris
(Copy No. 49)

DISTRIBUTION LIST FOR UNCL TM 72-109 (Cont'd)

Mr. A. Mitchell
Admiralty Research Laboratory
Teddington, Middlesex,
ENGLAND
(Copy No. 50)

Dr. P. Leehey
Department of Naval Architecture
Massachusetts Institute of Technology
77 Massachusetts Avenue
Cambridge, Massachusetts 02139
(Copy No. 51)

Stevens Institute of Technology
711 Hudson Street
Castle Point Station
Hoboken, New Jersey 07030
Attn: S. Tsakonas
(Copy No. 52)

Hamilton Standard
United Aircraft Corporation
Windsor Locks, Connecticut 06096
Attn: Mr. George Rosen
(Copy No. 53)

Dr. R. Mani
Assistant Professor
University of Massachusetts
131 Marston Hall
Amherst, Massachusetts 01002
(Copy No. 54)

Mr. N. J. Lipstein
General Electric R & D Center
Mechanical Engineering Laboratory
Schenectady, New York 12305
(Copy No. 55)

Mr. M. J. Benzakein
Manager
Adv. Acoustic Technology
General Electric Company
Cincinnati, Ohio 45215
(Copy No. 56)

Mr. F. F. Ehrich, Mgr.
Design Technology Operation
Aircraft Engine Group
General Electric Company
West Lynn, Massachusetts
(Copy No. 57)

Mr. B. D. Welliver
Unit Chief - Prop. Research
The Boeing Company
Seattle, Washington 98031
(Copy No. 58)

Mr. T. G. Sofrin
Pratt & Whitney Aircraft
East Hartford, Connecticut 06108
(Copy No. 59)

Mr. M. V. Lowson
Department of Transport Technology
Loughborough University of Tech.
Loughborough, Leics., ENGLAND
(Copy No. 60)

Mr. G. Sorran
Engineering Department
General Motors Corp.
Warren, Michigan 48089
(Copy No. 61)